NOISE, HOT CARRIER EFFECTS

Electric noise, or fluctuation in electric circuits, results from the discrete nature of charge carriers and their chaotic motion. Electric noise manifests itself as an acoustic noise in a telephone or a radio receiver, also as an irregular flickering on a television screen, known as a “snowfall” flicker, and otherwise. In general, fluctuations are temporary deviations of variables (current, voltage, resistance, frequency, etc.) either from their long-term averages or from some regular time-dependent values of information-bearing signals. This article deals with electronic noise caused by electrons and holes in semiconductors. For simplicity, the term electrons will be used, unless mentioning holes is necessary for specific reasons.

Fluctuations are best understood for electron gas which is in thermodynamic equilibrium with lattice vibrations. The universal relations of Nyquist and Einstein, together with Ohm’s law, interrelate noise, current, and other electronic transport, including electron diffusion. These relations are sufficient to estimate the ultimate accuracy for electrical measurements and signal processing under near-equilibrium conditions. However, advances in instrumentation and communication technology increasingly depend on progress in microelectronics, where deviations from equilibrium are essential, and the universal relations fail. High electric field enhances chaotic motion of electrons in devices and circuits. The customary name for this situation is *hot electrons.* Correspondingly, noise acquires features absent at equilibrium. Indeed, hot-electron noise differs from equilibrium, like a stormy sea differs from a mill pond. Measuring noise out of equilibrium provides new information about kinetic processes in electron gas—new as compared with that available from the average values of observables. As a result, investigation of hot electron noise proves to be a powerful tool for diagnosing nonequilibrium states in semiconductors subjected to high electric fields. Moreover, the obtained knowledge of the microscopic origin of hot electron noise helps to control it and suggests how to eliminate some sources of excess noise through improvement of material technology and circuit design, thus contributing to development of highly sensitive low-noise devices.

HOT-ELECTRON VELOCITY FLUCTUATIONS

Electric Noise at Equilibrium and in Nonequilibrium State

Fluctuations at Equilibrium. Fluctuations have been under investigation since 1827, when R. Brown published the results of his observations on the endless irregular motion of microscopic particles suspended in a liquid. Numerous sophisticated investigations of this phenomenon, called Brownian motion, led to the conclusion that the mean kinetic energies of a Brownian particle and a molecule of the liquid were equal, provided enough care was taken not to disturb their thermal equilibrium. Moreover, fluctuations of position of a Brownian particle were found closely related to the viscosity of the surrounding liquid and the force of friction acting on the particle. Experiments on Brownian motion and its theory, developed by A. Einstein and M. Smoluchowski, were important arguments in favor of the molecular-kinetic theory. The theory provided methodology to treat spreading of a cloud of particles (diffusion), friction, viscosity, and so on, in terms of velocity fluctuations. In particular, the Einstein relation associates the electron diffusion coefficient with electron mobility—the main electron transport parameter for a semiconductor in Ohm's law for current flow. Nyquist (1), in 1928, related the spectral density of current fluctuations in a resistor to the dissipative part of its conductance, or resistance. The Nyquist theorem and Einstein's relation together led to the fluctuation–diffusion relation, between electronic noise and electron diffusion.

In Nyquist's derivation one can also trace ideas of Rayleigh (1900), who applied the equipartition theorem to the standing-wave modes of black-body radiation. In some sense, the available noise power is a special low-frequency case of black-body radiation. Under proper matching, a resistor emits noise power into the matched transmission line connected to a radiometer—a sensitive device to measure radiation power. At thermal equilibrium, noise is white over a wide range of frequencies, that is, the spectral density of noise power does not depend on frequency and is the universal function of the absolute temperature. Thus, the noise radiometer serves as the absolute thermometer. (Visible and infrared radiation of a black-body is used to measure the absolute temperature as well.) Provided noise power differs from thermal power, the equivalent noise temperature (or, simply, noise temperature) is introduced, in order to estimate the deviation from equilibrium. The logarithmic ratio, in decibels, of the noise temperature over the absolute temperature is widely used for the same purpose.

In 1951, Callen and Welton (2) completed the theory of fluctuations at equilibrium by formulating the general fluctuation–dissipation theorem, which expresses the spectral density of fluctuations in a physical system at a given frequency, in terms of the dissipative part of the response of the system to some external perturbation. Accordingly, calculation, or measurement, of the system of linear response at a given frequency provides data on the spectral density of fluctuations of the corresponding variable at the same frequency. Consequently, measurement of electric noise at equilibrium gives no complementary information, as compared with that available from impedance measurements. On the other hand, measuring electron mobility and electron density in a semiconductor is sufficient to determine its noise properties at equilibrium.

The thermodynamic arguments collapse for an open system, subjected to a continuous energy flow, when some energy is supplied from the external world and then dissipated back to the external world. No universal relation is valid between noise and impedance in this case. This statement has fundamental and practical consequences. First of all, investigation of fluctuations from the nonequilibrium state is a valuable tool for diagnosis of different mechanisms of dissipation: relaxation of momentum, energy, intervalley transfer, as well as free-carrier number relaxation, which are reflected in the noise spectrum pattern of a biased semiconductor. On the other hand, the failure of the fluctuation–dissipation theorem allows, to a certain extent, independent control of the response and the noise through variation of the applied field, frequency, semiconductor doping, ambient temperature, sample length, and so on. Such a study, aimed at finding the favorable conditions for coexistence of high drift velocity and low excess noise, is important for the development of high-speed, low-noise devices.

Excess Noise at Low Electric Fields. Hot-electron effects are negligible in low electric fields, where the electrons easily dissipate energy gained from the applied electric field, and the electron temperature remains approximately equal to that of the semiconductor lattice. Nevertheless, electric current disturbs equilibrium and changes fluctuation spectra. For example, fluctuations of resistance (already present at equilibrium) cause no noise at zero bias, but they modulate current and manifest themselves in a biased semiconductor.

Many sources of excess electric noise, such as flicker noise, generation-recombination noise, and shot noise need current to appear (3–5). Flicker noise dominates at low frequencies, whereas generation-recombination noise is usually observed at intermediate frequencies. Shot noise is white over a wide range of frequencies. These sources of excess noise are not observed in directions transverse to the current. On the contrary, the noise resulting from electron velocity fluctuations is observed in all directions. It exceeds the flicker and generation-recombination noise at high frequencies.

Shot noise is important when the current is controlled by a barrier: a p–n junction, a Schottky barrier, a heterojunction, a tunneling structure, nonuniformities of doping, nonohmic contacts, and so on. The universal Schottky formula (6) say that, for shot noise, the spectral density of current fluctuations is proportional to the current. Measurement of noise characteristics as a function of current, frequency, and lattice temperature helps to distinguish different sources of excess noise, and suggests how to eliminate those of no interest. In particular, perfect ohmic contacts, uniform doping, and relatively high density of majority carriers, are prerequisites for avoiding interference of shot noise during experiments on hot-electron velocity fluctuations.

Electron Heating by Electric Field. A high electric field accelerates mobile electrons, and they accumulate excess energy. The steady state is reached when energy loss (usually at the lattice vibrations) compensates energy gain at a certain elevated mean energy of the electrons. The electron mean energy rising above its thermal equilibrium value—termed *hot electrons*—is specific to the electron behavior at high electric fields in semiconductors. The lattice temperature tends to increase as well, due to the Joule effect. However, the heat capacity of a semiconductor sample is much higher than that of the electron gas. Moreover, the lattice dissipates excess heat to the ambient, and the lattice temperature remains the same as (or only insignificantly higher than) the ambient temperature, provided a short voltage pulse is applied and the heat dissipation is efficient. The associated noise resulting from hot electrons is called hot-electron noise.

Hot-Electron Noise. Electronic processes inside the conduction band are fast, so the associated spectral features of excess noise appear at microwave frequencies. Therefore, it is quite natural that investigation of hot-electron noise at microwave and higher frequencies serves for diagnostics of fast and ultrafast processes in a semiconductor subjected to high electric fields. Microwave noise measurements usually deal with the noise power expressed in terms of the equivalent noise temperature. Another fluctuation characteristic is the spectral density of current fluctuations available from experimental data on noise temperature and small-signal microwave conductivity.

Experiments on hot-electron noise provide information on the anisotropy of kinetic energies in the longitudinal and transverse directions, the transverse and longitudinal diffusion coefficients of majority carriers, the energy relaxation time constant and its dependence on the applied electric field and lattice temperature, the intervalley transfer time constants for equivalent and nonequivalent valleys, and other important kinetic parameters of electronic processes inside the conduction and valence bands.

Kinetic Theory of Fluctuations from Nonequilibrium State

Toward the Price Relation. Kinetic theory of hot-electron fluctuations in semiconductors is an important part of physical kinetics (7). The crystal lattice presents an unperturbed thermal bath for the nonequilibrium electron gas in a semiconductor, allowing detailed treatment of hot-electron interaction with equilibrium phonons. This situation, and an understanding of the importance of fluctuations for the kinetic theory, immediately led to interesting results on hot electron fluctuations in semiconductors, reported by Lax (8), Price (9), Gurevich (10), Price (11), Gurevich and Katilius (12), Kogan and Shul'man (13).

In particular, Price (11) extended to hot electrons the fluctuation–diffusion relation between the spectral density of current fluctuations caused by electron velocity fluctuations and the diffusion coefficient associated with fluctuations of position of the same electrons. The Price relation was proven to hold, despite the failure of the Einstein relation, Ohm's law, and the Nyquist theorem for hot electrons.

General Theory. Later results, obtained for the case of frequent electron–electron collisions, contradicted the earlier results, and Gantsevich, Gurevich, and Katilius (14,15) and Kogan and Shulman (16) developed a self-consistent kinetic theory of fluctuations in a nonequilibrium case, based on the first principles of quantum mechanics and statistical physics. The theoretic apparatus of kinetic theory was generalized to obtain spectral properties of noise from statistical properties of collisions. The criteria of applicability of the theory were the same as for Boltzmann's equations used for response calculations. An important result obtained was (15) that the Price fluctuation–diffusion relation for hot electrons (11) had a narrower range of applicability than originally expected, with a high-density hot-electron gas being outside this range because of electron–electron collisions. The theory and its numerous applications to analytically tractable models are described in monographs (4,7) and review papers (17,18).

Hot-Electron Noise in Lightly Doped Semiconductors

Longitudinal and Transverse Noise. Developed theory and practical needs stimulated experimental investigation of hot-electron noise in semiconductors. Erlbach and Gunn (19) measured hot electron noise temperature for *n*-type germanium in the transverse direction to the current. The resultant increase of the transverse noise temperature with the applied electric field indicated that the electrons were hot. Bryant reported on longitudinal noise temperature for *n*-type GaAs (20). Avoiding possible contribution of generation-recombination noise, Bareikis, Vaitkevičiūtė, and Požela (21) measured the longitudinal noise temperature of hot carriers in *n*-type and *p*-type germanium (22) at microwave frequencies. Their study of longitudinal and transverse noise gave the first experimental evidence that noise temperature and spectral density of velocity fluctuations of hot carriers were anisotropic quantities. The experiment was performed on samples containing a relatively low density of hot carriers, and the results were interpreted in terms of the Price fluctuation–diffusion relation with the correct conclusion (21) that the diffusion coefficient of hot carriers was anisotropic as well. [Some time later, Wagner, Davis, and Hurst observed the anisotropy of electron diffusion in ordinary gases at high electric fields; see (23).] So, microwave noise experiments demonstrated the possibility to obtain results on field-dependent longitudinal and transverse diffusion coefficients for majority carriers in uniform samples without introducing carrier density gradients, and this technique (21,22) was applied to investigate hot-electron diffusion in the principal semiconductors used in electronics (24,25). The diffusion coefficient results obtained from microwave noise measurements were confirmed by experiments using other techniques [see (25)].

Fluctuations in One-Valley Semiconductors. The physics of noise relates the observed fluctuations in macroscopic variables to the microscopic processes inside a semiconductor. For hot-electron scattering by acoustic phonons in a one-valley semiconductor, theory predicted a negative convective contribution to longitudinal current fluctuations resulting from energy fluctuations (11,12). This phenomenon was experimentally confirmed in p-type germanium (22).

An essentially different contribution to longitudinal noise comes from inelastic scattering of hot electrons by optical phonons—the main energy loss mechanism at elevated electron energies. This scattering mechanism leads to resonant-type spectrum of velocity fluctuations in a narrow range of moderate electric fields at low lattice temperatures, as illustrated by experiments performed for p-type Ge and n-type InSb at 10 K lattice temperature [(26); see also (18)]. Optical phonon scattering, dominating over a wide range of electric fields in n-type GaAs and InP, leads to a broad and relatively weak noise source resolved at liquid nitrogen and room temperatures [see (24)].

Intervalley Fluctuations in Elementary Semiconductors. The conduction band of Ge and Si has several equivalent valleys, containing equal parts of the electron gas in equilibrium. An applied electric field introduces differences in the drift velocities and mean energies in the ellipsoidal valleys, oriented at different angles to the field, and the excess noise—hot-electron intervalley noise—appears (9). It is anisotropic, with respect to the electric field direction and to the crystallographic orientation (27). Intervalley noise and generation-recombination noise are examples of so-called partition noise [see (25)].

Intervalley Fluctuations in Compound Semiconductors. The conduction band of direct-band-gap compound semiconductors differs essentially from that of silicon and germanium. Equilibrium electrons occupy the lowest single valley, where their mobility is high. The upper low-mobility valleys are usually empty at equilibrium (except for high lattice temperatures), and a high electric field is needed for their occupation. Intervalley transitions of hot electrons cause longitudinal fluctuations of drift velocity. Intervalley noise of this type dominates in GaAs (28) and InP (29) at the subthreshold field for the Gunn effect. Sources of noise due to hot-electron transfer into satellite valleys located along the $\langle 111 \rangle$ and $\langle 100 \rangle$ directions (L- and X-valleys) were resolved in short submicrometer samples of n-type GaAs (30).

Monte Carlo Simulation of Fluctuations

Experimental studies demonstrate that hot-electron noise characteristics are sensitive to subtle details of the semiconductor band structure and scattering mechanisms. This stimulates the interpretation of experimental data, in terms of realistic semiconductor models. While analytical models perfectly illustrate the kinetic theory with deep insight into the physics of hot-electron noise, numerical techniques are useful in extracting quantitative information on the dominant kinetic processes inside the conduction band.

Simulation of Hot-Electron Fluctuations. The Monte Carlo method—a versatile numerical technique—introduces hot-electron velocity fluctuations into the simulation procedure in a natural way. The first calculation of hot-electron noise spectra by the Monte Carlo technique (31) was immediately followed by a paper (32), in which a better estimate of the scattering parameters of holes in the valence band of germanium was obtained by fitting the Monte Carlo simulation data to the experimental results. Simulation techniques and calculation of the spectral properties of hot-electron noise are described in a monograph (33) on Monte Carlo methods and their application to semiconductor devices. Recent developments and results with emphasis on hot-electron noise in semiconductor structures are discussed in review papers (34–36). This Monte Carlo approach applies at low electron densities, and modified procedures are needed to treat fluctuations when electron–electron collisions are essential (37–39).

Simulation of Hot-Electron Diffusion. The Price fluctuation–diffusion relation, valid at low electron densities, provides another possibility to compare experimental data on hot-electron velocity fluctuations and numerical results for realistic models. Motion of individual electrons in real space, resulting in diffusive spreading of an electron cloud, was simulated by the Monte Carlo technique, and the diffusion coefficient available from this simulation was compared with data on spectral density of current fluctuations available from microwave noise measurements [see (24,25)].

Effect of Electron–Electron Collisions

Electron–electron collisions are energy and momentum conserving; they have no direct effect on energy and drift velocity, but do influence these averages through other scattering mechanisms. For example, an electron–electron collision can assist emission of an optical phonon by one of the electrons supposing that each electron lacks energy for the emission before the collision. The associated loss of energy is essential. It causes a slow increase of hot electron noise temperature at moderate electric fields and cryogenic temperatures, as illustrated by comparing the results of Monte Carlo simulation with the experimental data for n-type GaAs (39). Moreover, theory predicts that two-carrier collisions in hot-electron gas create additional correlation, and the additional term enters the fluctuation–diffusion relation (15) [see also (37)].

Semiconductor Structures

Short Channel Effects. Modern microelectronics is shaped by small-size and low-dimension semiconductor structures. Investigation of hot-electron noise in such structures is important when one tries to minimize the associated excess noise at high speed of operation. Hot electrons fail to reach the steady-state, corresponding to an infinitely long sample, provided the sample is short and the hot electrons leave the sample for the electrode early enough. As a result, a higher electric field is needed for the intervalley noise to appear in short samples (37). In other words, at a fixed electric field, the intervalley noise is suppressed in short channels. The essential suppression of hot-electron noise in short channels has been demonstrated for lightly doped n-type GaAs (40) and InP (41), and for standard-doped n-type GaAs (42). For a comparison with the results of Monte Carlo simulation, see Ref. (24).

Two-Dimensional Electron Gas Channels. In two-dimensional electron gas (2-DEG), the electrons are free to undergo planar motion, but their transverse freedom is limited by the heterojunction and electrostatic barriers. The degree of transverse freedom depends on the barrier height and the electron kinetic energy, the latter being easily controlled by the electric field applied in the plane of electron localization. This introduces sources of excess noise specific to low-dimensional channels (43,44). Dependence of hot-electron noise on channel length is also important for low-noise operation of 2-DEG channels at microwave frequencies (44).

THEORETIC BACKGROUND

Hot-electron fluctuations depend on the details of kinetic processes taking place in a biased semiconductor. This requires consideration of the values in the nonequilibrium spectra that reflect these details. Definitions and relations appropriate for the nonequilibrium state and converging to the equilibrium states at zero bias are introduced in this section.

Correlation Function and Spectral Density of Fluctuations

Electric current in a semiconductor sample results from motion of the mobile electrons present in the sample. Random motion of individual electrons produces fluctuations of the current, $\delta\mathbf{I}(t)$, around the time-independent mean value $\overline{\mathbf{I}}$. Let us consider N electrons in a uniform sample under steady-state, reached in a uniform static electric field $\mathbf{E}$. The time-dependent velocity of the all-electron mass center, averaged over the mobile electrons, or drift velocity, is

$$\mathbf{v}_d(t) = \frac{1}{N}\sum_{n}^{N}\mathbf{v}_n(t) \tag{1}$$

where $\mathbf{v}_n(t)$ is the instantaneous velocity of the n-th electron and t is time. Fluctuations of the drift velocity $\delta\mathbf{v}_d(t)$ around the time-independent mean value $\overline{\mathbf{v}_d(t)}$ are present in all directions:

$$\delta\mathbf{v}_d(t) = \mathbf{v}_d(t) - \overline{\mathbf{v}_d(t)} \tag{2}$$

The bar here and in the following designates the average over time. The fluctuating time-dependent drift velocity for a chosen model can be obtained from Monte Carlo simulation [see (33)].

The quantity that yields important physical information on the size of the fluctuations and how they decay in time is the drift velocity autocorrelation function (see Ref. 4). In the direction of interest, the autocorrelation function is

$$\Phi(\tau) = \overline{\delta v_d(t)\delta v_d(t+\tau)} \tag{3}$$

where τ is the time difference between two observations, and $v_d(t)$ is the drift velocity component in the chosen direction. The autocorrelation function value $\overline{\delta v_d^2(t)}$ at $\tau = 0$ is called variance. Correlation functions are available from the equations of fluctuation kinetics or from Monte Carlo simulation (see Refs. 17,18,33,34).

Fourier transformation of the drift velocity autocorrelation function [Eq. (3)] gives the spectral density of drift velocity fluctuations in the direction of interest (Wiener–Khintchine theorem) (see Ref. 3).

$$S_v(\omega) = 4\int_0^{\infty}\Phi(\tau)\cos(\omega\tau)\,d\tau \tag{4}$$

Electron velocity fluctuations induce voltage fluctuations on the sample terminals and current fluctuations in the circuit. It is a convention to deal with the open-circuit voltage fluctuations and the short-circuit current fluctuations unless otherwise mentioned. The current which is usually measured outside the sample can be related to the electron drift velocity inside the sample. In a similar way, the current fluctuations can be expressed in terms of the drift velocity and other fluctuations. In general, the relation is complicated, but it acquires a simple form in the case of a uniform electric field in a uniformly doped sample of constant cross-section at high frequencies where electron number fluctuations can be ignored. Hence, the spectral density of current fluctuations S_I is proportional to that of drift velocity fluctuations

$$S_I(\omega) = e^2 n S_{\mathrm{v}}(\omega)\ Q/L \tag{5}$$

where e is the elementary charge, n is the electron density, Q is the cross-section area, L is the sample length (interelectrodal distance), ω is the circular frequency, and S_{I} is determined in A^2 s. Discussion of more complicated cases can be found elsewhere (34,36,45).

In general, the spectral density of current fluctuations is a tensor quantity, consisting of three diagonal and six off-diagonal components. A diagonal component results from the autocorrelation function of the time-dependent drift velocity component along the corresponding Cartesian axis [see Eq. (3)]. An off-diagonal component comes from the velocity covariation function [of a similar form as Eq. (3)], but containing the product of the time-dependent drift velocity components along two Cartesian axes. In an isotropic medium, for example, in an amorphous solid, the tensor of spectral density can be reduced to three diagonal non-zero components, the parallel to the applied electric field component and two transverse components, the latter two being equal to each other. In crystals, for example Si or Ge subjected to electric field, the off-diagonal components are also important.

Available Noise Power and Noise Temperature

Hot-electron velocity fluctuations and associated fluctuations of current dominate over other sources of fluctuations at microwave frequencies. The fluctuating, that is, time-dependent current, causes emission of electromagnetic waves into an open space or into the load (a coaxial cable, a waveguide, a coplanar line, etc.). Therefore, the semiconductor sample feeds the power into the load. The emitted noise power is of special importance in this frequency range, since the current fluctuation spectra (directly available from the velocity fluctuation spectra, in theory) are not measured at microwave frequencies directly. It is a convention to consider the emitted/absorbed noise power for matched impedances of the sample and the load, unless stated otherwise. Under this condition, the noise power is called the power available at the noise source or the available noise power.

The available noise power $P_n(f)$ emitted by a source of noise in a fixed frequency band Δf around a frequency $f = \omega/$

2π can be estimated by comparing it with the power radiated into the same frequency band by an absolutely black body kept at a known temperature. In case of equal powers at a given frequency, one can say that the equivalent noise temperature of the noise source at this frequency equals the absolute temperature of the reference black body. The equivalent noise temperature, or noise temperature, $T_n(f)$, multiplied by the Boltzmann constant k_B is, by definition, the power, per unit frequency band around the frequency f, dissipated by the sample into the matched load (see Ref. 4):

$$T_n(f) = \frac{P_n(f)}{k_B \Delta f} \tag{6}$$

Hot-electron noise power depends on frequency, direction, electric field, and so on. This forces one to introduce frequency-, direction- and field-dependent equivalent noise temperature. In an isotropic medium, the nonequilibrium noise temperature differs in the directions parallel and transverse to the current. The hot-electron noise temperature, $T_n(f)$, represents a property of an electron gas differing from its energy temperature T_e, which is defined on the basis of the electron average energy, $T_e = (2/3)\langle\epsilon\rangle/k_B$.

In equilibrium, the noise temperature of the sample in question is independent of frequency over the wide range of frequencies, and equals the absolute temperature: $T_n = T_0$. The equilibrium noise spectrum is white [until $\hbar\omega \ll k_B T_0$, see Ref. (41)], and the available noise power in this range of frequencies can serve for establishment of the absolute scale of temperature.

Spectral Density of Current Fluctuations and Noise Temperature

Noise power can be expressed in terms of spectral density of current fluctuations and impedances of the sample and the load. For the matched impedances one has:

$$P_n(f) = \frac{1}{4} S_I(f) \mathrm{Re}\{Z(f)\} \Delta f \tag{7}$$

where S_I is the spectral density of current fluctuations determined under the short-circuit condition, and $Z(f)$ is the ac impedance of the sample around the dc bias point. (The matching of the sample and the load means that their impedances are equal.)

From Eqs. (6) and (7), the spectral density of short-circuit current fluctuations for hot electrons in a sample subjected to electric field E can be related to the noise temperature and the sample impedance:

$$S_I(f, E) = \frac{4 k_B T_n(f, E)}{\mathrm{Re}\{Z(f, E)\}} \tag{8}$$

where S_I, T_n and Z are determined in a chosen direction (e.g., longitudinal or transverse to the electric field E for isotropic semiconductors). Thus, measurement of the impedance and the noise temperature are sufficient to obtain the experimental short-circuit value of current fluctuation spectral density for hot electrons. Since the same quantity is available from theory [see Eq. (5)], a comparison of the experimental data with the results of calculation is possible.

Voltage fluctuations are seldom considered at microwave frequencies. For completeness, note that the spectral density of voltage fluctuations on the sample terminals for the open circuit and the spectral density of current fluctuations under the short-circuit condition are interrelated, according to $S_V(f) = |Z(f)|^2 S_I(f)$.

Fluctuation–Dissipation Theorem and Its Extension

The Nyquist Theorem. As discussed above, the noise temperature at equilibrium equals the absolute temperature. Hence, for equilibrium it follows, from Eq. (8):

$$S_I(f) = 4 k_B T_0 / \mathrm{Re}\{Z(f)\} \tag{9}$$

This relation is called the *Nyquist theorem* in the classical limit ($\hbar\omega \ll k_B T_0$). A sophisticated derivation of the Nyquist theorem can be found elsewhere (4).

The Einstein Relation. At equilibrium, the electron mobility and the diffusion coefficient are closely related according to the Einstein relation. For low-density nondegenerate electron gas, the relation is simplified to:

$$D_0 = \mu_0 \frac{k_B T_0}{e} \tag{10}$$

where μ_0 is the low-field low-frequency electron mobility and D_0 is the zero-field diffusion coefficient in the expression for the diffusion current density, $j_d = -eD_0 \nabla n$, resulting from the electron density gradient ∇n.

Lorentz-Type Spectrum. The principle of energy equipartition means that the equilibrium mean energy contained in every degree of freedom equals $k_B T_0/2$. Applied to the mean energy of the all-electron mass center at equilibrium, the principle relates the drift velocity fluctuation variance in the direction of interest to the temperature:

$$Nm\overline{v_d^2(t)} = k_B T_0 \tag{11}$$

where m is the electron effective mass.

For a rectangular sample, the variance of current at equilibrium can be presented as

$$\overline{I^2(t)} = e^2 N^2 \overline{v_d^2(t)} / L^2 = \frac{e^2 N}{mL^2} k_B T_0 \tag{12}$$

This equation relates equilibrium fluctuations of the current component in a given direction to the absolute temperature.

The electron momentum relaxation time, τ_p, in the simple expression for the low-field electron mobility,

$$\mu_0 = (e/m)\tau_p \tag{13}$$

determines the decay of corresponding fluctuations

$$\overline{\delta I(t)\delta I(t+\tau)} = \overline{\delta I^2} e^{-\tau/\tau_p} \tag{14}$$

Integration [see Eq. (4)] yields the frequency dependence of the spectral density of current fluctuations at equilibrium

$$S_I(\omega) = 4\int_0^\infty \overline{\delta I^2} e^{-\tau/\tau_p} \cos(\omega\tau)\, d\tau = \overline{\delta I^2} \frac{4\tau_p}{1 + \omega^2 \tau_p^2} \tag{15}$$

A spectral dependence like this is called a Lorentz spectrum.

Equations (12) and (15) lead to the Nyquist relation

$$S_I(\omega) = 4k_B T_0 eN \,\mathrm{Re}\{\mu(\omega)\}/L^2 \tag{16}$$

where the real part of ac mobility $\mu(\omega)$ is introduced:

$$\mathrm{Re}\{\mu(\omega)\} = \frac{(e/m)\tau_p}{1+\omega^2\tau_p^2} \tag{17}$$

The electron mobility μ (determined by the momentum relaxation time constant τ_p) and the electron density n are the most important parameters of electron transport in semiconductors. According to the Nyquist relation, in the form of Eq.(16), the same parameters decide noise at equilibrium.

Fluctuation–Diffusion Relation. Velocity fluctuations of individual electrons cause fluctuations of their positions, resulting in diffusive spreading of a cloud of electrons, diffusion current, and other diffusion phenomena. As a result, an important relation exists between the diffusion coefficient and the spectrum of current fluctuations. Using the Einstein relation [Eq. (10)] and the Nyquist theorem [Eq. (16)] for $\omega\tau_p \ll 1$, one obtains [see Eq. (5)]:

$$S_v(0) = 4D_0 \tag{18}$$

So, the basic kinetic coefficients (mobility, diffusion coefficient) and spectral density of velocity fluctuations are interrelated through Nyquist [Eq. (16)], Einstein [Eq. (10)], and fluctuation–diffusion [Eq. (18)] relations at thermal equilibrium. Measurements or calculation of velocity fluctuation characteristics at equilibrium give no additional information not already available from the mobility.

Beyond the Fluctuation–Dissipation Theorem

Calculation of hot-electron noise is an independent problem of kinetic theory, which cannot be reduced to the calculation of the response of an electron system to external deterministic perturbation. So, in general, knowledge of the sample impedance is not sufficient for determination of excess noise. Nevertheless, under well-defined conditions, some useful relations can be applied to hot-electrons in a biased semiconductor.

The Price Relation. Price (10) generalized the fluctuation–diffusion relation for a semiconductor subjected to a high electric field under the following conditions: (1) the system is electrically stable, that is, $\mathrm{Re}\{\mu(E,f)\} > 0$, (2) two-carrier interaction is neglected, (3) the thermal bath is not perturbed, (4) the electronic processes in the conduction band are essentially faster than those including energy levels in the gap (electron trapping) and the valence band (electron-hole recombination). It turns out that, as for the thermal equilibrium, the fluctuation–diffusion relations are valid for hot electrons:

$$(S_v)_{xx} = 4D_{xx} \tag{19}$$

$$(S_v)_{xy} = 2(D_{xy} + D_{yx}) \tag{20}$$

where S_v stands for the tensor components of drift velocity fluctuation spectral density in the frequency range, where the maximum contribution comes from all intraband electronic processes.

Equations (19) and (8) lead to the equivalent form of the Price relation:

$$D_{xx}(E) = \frac{1}{e}k_B T_{nx}(E)\cdot \mathrm{Re}\{\mu_{xx}(E)\} \tag{21}$$

where the hot-electron noise temperature T_{nx} is determined in the direction x, the electric field E being applied in any direction. The corresponding diagonal component of the real part ac mobility tensor, μ_{xx}, is determined at frequencies low, compared with the inverse time constants of the momentum relaxation and other relaxation processes inside the conduction band.

The Price relation is valid for hot electrons even when the Ohm, Einstein, and Nyquist relations do not hold. It is a useful relation for low-density, hot-electron gas, in contact with an unperturbed thermal bath of a semiconductor. The relation has suggested a convenient way to measure the components of the diffusion coefficient tensor for hot electrons, without introducing electron density gradient (21).

Further on, the diagonal components in the longitudinal and transverse directions to the applied electric field will be discussed (let the field be directed along the x-axis): $(S_v)_\parallel = (S_v)_{xx}$ and $(S_v)_\perp = (S_v)_{yy}$.

Additional Correlation Due to Electron–Electron Collisions. The Price relation has been generalized (15) into:

$$\mathbf{S}_v = 4(\mathbf{D} + \boldsymbol{\Delta}) \tag{22}$$

where $\boldsymbol{\Delta}$ is the tensor resulting from the additional correlation caused by the inter-electron collisions (15) (see also Refs. 17,18,37). The additional correlation arises only at nonequilibrium conditions, disappearing at equilibrium.

Excess Noise in Electron Temperature Approximation. Frequent electron–electron collisions establish hot-electron distributions governed by the electron temperature. In the electron temperature approximation for quasielastic scattering, the kinetic theory of fluctuations allows one to express the noise temperature in terms of conductivities, and lattice T_0 and electron T_e temperatures (13):

$$(T_n)_\perp = T_e \tag{23}$$

$$(T_n)_\parallel = T_e\left[1 + \frac{T_e}{4(T_e - T_0)}\left(\frac{\mu_\parallel}{\mu_\perp} + \frac{\mu_\perp}{\mu_\parallel} - 2\right)\right] \tag{24}$$

where $(T_n)_\parallel$ and $(T_n)_\perp$ are the longitudinal and transverse noise temperatures, $\mu_\parallel$ and $\mu_\perp$ are the longitudinal and transverse ac mobilities. Equations (23) and (24) hold at low microwave frequencies $\omega \ll \tau_\epsilon^{-1}$, provided the electron–electron collisions control the electron distribution in energy: $\tau_p \ll \tau_{ee} \ll \tau_\epsilon$ (here τ_{ee}^{-1} is the frequency of the interelectron collisions). It is noteworthy that the longitudinal excess noise depends on the small-signal mobilities in the longitudinal and transverse directions, this dependence disappearing in absence of hot electron effects: when either $T_e = T_0$ or Ohm's law holds and $\mu_\perp = \mu_\parallel$. One can notice a possible simplification at high electric fields, where $T_e \gg T_0$, the resultant expression demonstrating the same complex dependence on the deviations from Ohm's law.

Examples of Hot Electron Fluctuation Spectra

In the previous section the main concepts, definitions, and important theoretic results on fluctuations near a nonequilibrium state were presented in the limit of low microwave frequencies. This section presents some examples of possible spectra of spatially homogeneous current fluctuations (for more details, see Ref. 18).

Convective Noise. Energy fluctuations contribute to fluctuations of current in the direction of a steady-current. The contribution is easy to resolve in one-valley semiconductors in case of quasielastic scattering. Quasielastic scattering means that a collision changes the direction of the electron motion remarkably, with little effect on the absolute value of the electron velocity. The well-known example is electron scattering by acoustic phonons at not too low lattice temperatures: many collisions are needed for energy relaxation, so two time constants decide relaxation of fluctuations. They are the momentum relaxation time, τ_p, and the energy relaxation time, τ_ϵ, the latter being larger than the first.

The spectral density of longitudinal current fluctuations in the presence of an external electric field contains the term due to energy fluctuation, resulting in the so-called convective contribution to noise (11,12)

$$S_I(\omega, E) = \frac{4\overline{\delta I^2}\tau_p}{1+\omega^2\tau_p^2} + \frac{C}{1+\omega^2\tau_\epsilon^2} \tag{25}$$

where C is the low-frequency ($\omega\tau_\epsilon \ll 1$) limit of the convective term. The latter is important, provided Ohm's law does not hold. The sign of deviation from Ohm's law decides the sign of C (12,16): $C < 0$ in case of a sublinear current–voltage characteristic, and $C > 0$ for a superlinear one. The mobility decreases with increasing electron energy in lightly doped semiconductors. In this case, the convective contribution causes the partial suppression of current fluctuations in the longitudinal direction at frequencies $\omega\tau_\epsilon \sim 1$.

Intervalley and Real-Space Transfer Noise. In many-valley semiconductors the total number of electrons consists of the partial numbers corresponding to different valleys. Fluctuations of occupancies modulate the current and cause current fluctuations. Price (8) introduced the term *intervalley noise* to account for the extra contribution arising from the occupancy fluctuations.

Assuming that the intravalley processes are fast, as compared with the intervalley processes, the spectral density of velocity fluctuations in a chosen direction for a simple two-valley model can be written as

$$S_v(\omega, E) = \frac{\overline{n}_1}{n}S_1 + \frac{\overline{n}_2}{n}S_2 + 4\frac{\overline{n}_1\overline{n}_2}{n^2}(\overline{v}_1 - \overline{v}_2)^2\frac{\tau_i}{1+(\omega\tau_i)^2} \tag{26}$$

where τ_i is the intervalley relaxation time constant (inversely proportional to the squared intervalley coupling constant), n is the electron density, while $\overline{n}_1$, $\overline{v}_1$, S_1 and $\overline{n}_2$, $\overline{v}_2$, S_2 are the average electron densities, drift velocities, and spectral densities of velocity fluctuations in valleys of type 1 and 2, respectively. Consequently, hot electron noise in a many-valley semiconductor is not equal to the sum of the corresponding intravalley contributions weighted by the partial numbers of electrons. The last term in Eq. (26) is always positive; it vanishes in two cases: for equivalent valleys, when $\overline{v}_1 = \overline{v}_2$, and at thermal equilibrium, when $\overline{v}_1 = 0$ and $\overline{v}_2 = 0$. Thus, current is necessary for the contribution from intervalley fluctuations, but electron heating is not necessary, in general. For example, at a relatively high lattice temperature, the transitions between nonequivalent valleys can lead to intervalley noise at low electric fields, without electron heating.

From Eqs. (19) and (26) one obtains a simplified expression for the intervalley diffusion

$$\Delta D = \frac{\overline{n}_1\overline{n}_2}{n^2}(\overline{v}_1 - \overline{v}_2)^2\tau_i \tag{27}$$

Expressions given by Eqs. (26) and (27) are also suitable to describe excess noise and diffusion caused by transverse electron transitions from one layer to another in semiconductor structures containing layers with different electron mobilities. The related noise, appearing in the longitudinal direction, is called real-space-transfer noise.

EXPERIMENTAL TECHNIQUES

Noise spectroscopy, unlike the usual optical one, deals with relaxation, that is, aperiodic processes. Different electronic processes, characterized by relaxation times τ_m, cause steps at frequencies around $\omega\tau_m = 1$. Each step has a simple Lorentzian form, provided the decay of fluctuations is exponential. As mentioned, hot-electron noise results from the kinetic processes taking place inside the conduction band. Their relaxation times are in the picosecond and subpicosecond range. Therefore, microwave and higher frequencies serve best for experimental investigation of hot-electron fluctuation spectra. In this range of frequencies, other sources of noise, such as $1/f$ fluctuations, generation-recombination noise, and the like, do not mask hot-electron effects.

General Requirements

Samples. A semiconductor sample for hot-electron noise measurements at microwave frequencies is a nonlinear resistor. A typical shape is a rectangular parallelepiped, with two ohmic electrodes at its bases. For investigation of epitaxial conductive channels, coplanar ohmic electrodes are more convenient. The epitaxial sample is cut from a transmission-line-model structure. A standard coplanar configuration with different interelectrodal distances (often exploited to estimate contact resistance) is quite acceptable. Longitudinal and transverse noise temperatures can be measured by placing the sample oriented either normal or parallel to the wide walls of the waveguide. Fluctuations of current excite the H10 mode in the waveguide, and the ac electric field of the emitted noise, depending on the sample orientation, is either parallel or transverse to the bias field.

On-wafer microwave noise measurements can be performed using microprobes. Each microprobe consists of a central wire and two side wires attached for screening. Microprobes are connected to hard coaxial lines or waveguides, and are put in contact with the sample electrodes on the wafer.

Pulsed Measurements of Hot-Electron Noise. Spectral analyzers are now commercially available for a wide range of frequencies up to and including the V-band of millimeter waves. They operate in a cw mode and support standard cw measurements of noise in semiconductor devices in many laboratories. However, investigation of hot-electron effects and other effects at high electric fields require pulsed rather than cw modes of operation. Pulsed measurements help to avoid thermal walkout, due to the Joule effect prevailing in a cw mode. The increase in the lattice temperature masks hot-electron effects. Unfortunately, spectral analyzers for pulsed measurements are not commercially available yet, and radiometric techniques operating at fixed frequencies are used to obtain the data specific to hot electrons. The noise power in the chosen frequency band Δf at frequency f is selected by a filter, then amplified and fed into a radiometer for noise power measurement.

Waveguide and Coaxial Techniques. Pulsed measurements of noise power impose several special requirements. The noise must be measured when the electric field is on, that is, the radiometer is opened for a short time. One has to deal with a low and extremely short noise signal in the presence of high pulsed voltage, the latter penetrating into the noise-measuring circuit and disturbing the sensitive amplifier, unless the radiometric circuit is safely decoupled from the one which is used to heat the electrons. The decoupling is easily achieved at microwave frequencies. This frequency range is also useful for another reason: Flicker and generation-recombination noise sources are cut off at microwaves and do not interfere with hot-electron noise measurements.

Measurement at high electric fields introduces a problem: the electric field changes the sample impedance and causes a mismatch of the sample to the load—the transmission line connecting the sample to the radiometer. The mismatch must be eliminated by changing the load impedance.

These problems have been solved by developing a waveguide-type short-time-domain gated modulation radiometer (47). Low transmission losses in waveguides narrow-band low-noise, high-gain parametric microwave amplifier available at microwave frequencies, efficient filtering-out of parasitic signals, make a waveguide-type radiometer a valuable instrument for research of hot-electron fluctuations [see (18,24)].

Coaxial techniques have also been widely used (19,20,27,29) (see also Ref. 24). The coaxial technique, using a wide-band amplifier, appropriate filters, and pulsed bias, assures measurement of hot-electron noise over a wide range of frequencies, without changing the sample-holder hardware.

Waveguide-Type Short-Time-Domain Gated Radiometer

Radiometric Setup. Figure 1 presents a schematic view of the radiometric setup for hot-electron noise measurements at microwave frequencies. The experimental procedure for determining the noise temperature T_n consists of two steps.

The first step is the measurement of the current–voltage characteristic and matching the waveguide impedance to that of the sample at each bias. The bias voltage pulses are typically from 1 μs to 5 μs duration, fed at a 125 Hz repetition rate. The master generator 3 drives the pulse voltage generator 2 and the microwave generator 4. When microwave switch 7 (Fig. 3) is connected to port 7a, the microwave generator 4, the microwave line 5, and the transformer 8 are used to match the sample, that is, to reach the minimum standing microwave ratio. The resistance bridge 9 controls the sample resistance at each bias level.

The second step is the noise temperature measurement of the sample at a chosen bias. The switches 7 and 11 are connected to ports 7b and 11a, respectively. The noise signals from the sample 1 and the reference noise generator 13 are periodically fed into the input of the gated modulation radiometer, which is opened twice during the period of modulation: first, to connect the biased sample 1 to the radiometer, and for the second time to connect the reference noise generator 13. The difference between the signal levels is used to determine the noise temperature of hot electrons. The delay of the gating pulse ensures the noise power measurements before, during, and after the voltage pulse, if necessary. This is sufficient to control the channel overheat. The best matching

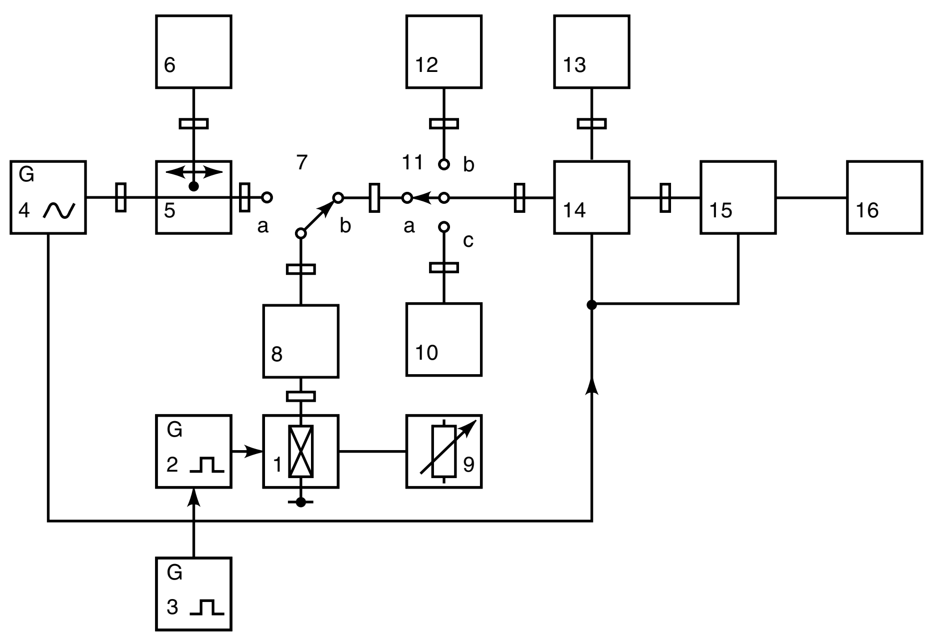

Figure 1. A schematic setup for hot-electron microwave noise power measurements: 1—the investigated sample in the waveguide; 2—the pulsed voltage generator; 3—the master generator; 4—the microwave generator; 5—the microwave line; 6—the SWR indicator, 7, 11—the microwave switches; 8—the impedance transformer; 9—the resistance bridge; 10, 13—the reference noise generators at T_0 = 293 K; 12—the reference noise generator at $T = (T_0 + 200)$ K; 14—the modulator; 15—the gated modulation radiometer; 16—the indicator.

data (transformer data) obtained for each bias are used. The standard noise reference sources 10 and 12 are connected to check the zero level (switch at port 11c) and the gain of the radiometer amplifiers (port 11b). The limit parameters of the X-band radiometer with 10^{-7} s gating time are as follows: the power sensitivity 10^{-15} W, the systematic error 0.25 dB, the noise temperature range up to 100 $k_B T_0$.

Measured and Available Noise Power. The measured noise power data are sufficient to determine the available noise power, provided the sample is matched to the waveguide and the waveguide losses (and the associated waveguide related noise) are negligible. Since the sample impedance is field-dependent, the optimal conditions are not achieved over the wide range of electric field values. Losses and mismatch are corrected by additional microwave measurements.

Small-Signal Response and Current Fluctuations. The spectral density of current fluctuations $S_I(E)$ is determined from the data on noise temperature $T_n(E)$ and small-signal ac conductance $\mathrm{Re}\{Y(E)\}$ of the sample, according to Eq. (8). Let us give a brief description of the technique to measure $\mathrm{Re}\{Y(E)\}$, operating at the pulsed bias and using the same sample mounting, which is compatible with the gated radiometer. First, the standing wave ratio $K(E, B = 0)$ is measured at a strong electric field E at zero magnetic field at the ambient temperature. Then, the electric field is switched off, and the previous value of the standing wave ratio is reached at zero electric field $K(E = 0, B) = K(E, B = 0)$, by changing the sample conductance with external magnetic field B or by changing the lattice temperature. Now, the dc low-field conductance is measured in the standard way, at a very low dc electric field. Since a strong inequality holds at microwave frequencies, $(\omega\tau_p)^2 \ll 1$, one has: $Y(\omega = 0, E = 0, B) = \mathrm{Re}\{Y(\omega, E = 0, B)\}$, where $Y(\omega, E = 0, B)$ is the zero-field ac admittance at the microwave frequency in the magnetic field. The equality of the standing wave ratios means that the small-signal microwave ac impedances are also equal, and $\mathrm{Re}\{Y(\omega, E, B = 0)\}$, $= Y(\omega = 0, E = 0, B)$. Therefore, the required small-signal conductance at the microwave frequency under strong pulsed electric field E is available from the zero-field dc conductance, measured at a low electric field. This technique allows one to determine the small-signal conductance at the microwave frequency in the direction parallel and transverse to the bias field E.

Extremely High Electric Fields in Conductive Channels. Experimental study of hot-electron noise in conductive channels at extremely high electric fields is hindered by host crystal heating and thermal breakdown. A technique was developed to perform the measurements at fields up to the impact ionization threshold (30). A nanosecond/microwave sample holder was designed to perform short-time-domain pulsed measurements of hot-electron noise power at microwave frequencies. The sample was placed into the coaxial part of the holder, enabling the application of 100 ns pulses of electric field along the channel. For coupling the investigated channel to the waveguide, a T-shaped antenna was used. Matching of the channel circuit to the waveguide was controlled by the standing-wave-ratio meter. The noise power emitted by the channel into the waveguide was compared with that of the "black body" radiation source kept at known temperature. This technique was applied to measure the equivalent noise temperature of hot electrons in the channel in the direction of the applied electric field. The average fields up to 300 kV/cm were reached in standard doped ungated GaAs channels for field effect transistors.

EXPERIMENTAL RESULTS ON HOT-ELECTRON NOISE

Failure of the fluctuation–dissipation relation at nonequilibrium conditions means that spectra of noise are rich, contain many features, and knowledge of electron density and mobility is not sufficient to predict noise characteristics of a particular semiconductor subjected to a high electric field. Detailed information on excess noise is available, either from noise measurements or from realistic model calculations. This article contains the experimental results selected to illustrate the most specific effects of hot electrons on excess noise.

Anisotropy of Hot Carrier Noise

Longitudinal and Transverse Noise Temperature. Hot-electron noise temperature T_n is an anisotropic quantity. The directions parallel and transverse to the steady current are not equivalent, even in the simplest case of a spherically symmetric band structure and isotropic scattering mechanisms. This is illustrated in Fig. 2, which presents the noise temperatures measured for p-type germanium at 9.6 GHz frequency and 80 K lattice temperature (21). The origin of the transverse noise temperature is similar to that at equilibrium—it is closely related to the hole kinetic energy. Therefore, the measured transverse noise temperature gives experimental evidence that the holes become hot when subjected to a high electric field. This effect is not masked by contributions from the fluctuations that modulate the steady current flow and appear in the longitudinal direction.

Transverse Noise Temperature and Energy Relaxation. For a simple band structure in the carrier temperature approximation, the transverse noise temperature equals the carrier temperature, the latter being determined by the mean energy of carriers [see Eq. (23)]. Monte Carlo simulation shows this to be approximately true for holes in p-type germanium (31), where

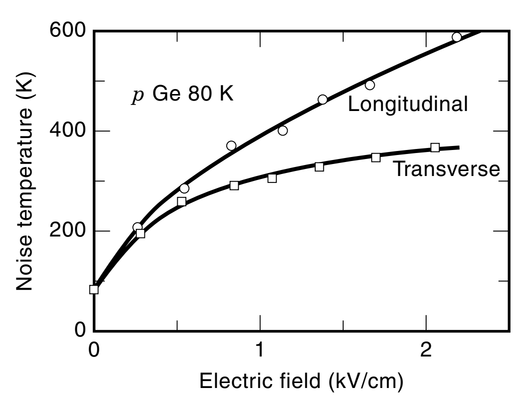

Figure 2. Equivalent noise temperature of hot holes increases with applied electric field in different ways when measured in the longitudinal and transverse directions to the steady current. Experimental data for p-type germanium (22) ($p = 1.5 \cdot 10^{14}$ cm^{-3}, $T_0 = 80$ K). Solid curves are guides to the eye.

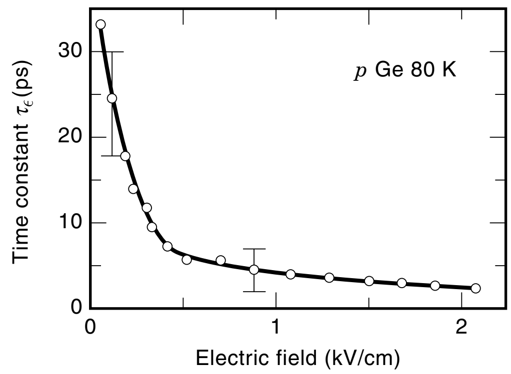

Figure 3. Hot-hole energy relaxation time constant τ_ϵ in p-type germanium, deduced from the transverse noise temperature measured in the ⟨110⟩ direction for electric field applied in ⟨$1\bar{1}0$⟩ direction (48). The time constant decreases as the electric field increases. Solid curve is a guide to the eye. $p = 1.5 \cdot 10^{14}$ cm^{-3}, $T_0 = 80$ K.

measurements of the transverse noise temperature can serve for estimation of the mean energy of hot holes, $\langle\epsilon\rangle \approx (3/2)k_B (T_n)_\perp$, and of the energy relaxation time constant τ_ϵ:

$$\tau_e = \frac{\langle\epsilon\rangle - \langle\epsilon_0\rangle}{e(\overline{\mathbf{v}}_d\mathbf{E})} \approx \frac{3}{2}\frac{k_B((T_n)_\perp - T_0)}{e(\overline{\mathbf{v}}_d\mathbf{E})} \tag{28}$$

Figure 3 presents the dependence on the applied electric field of the energy relaxation time constant obtained for p-type Ge, according to Eq. (28) from the experimental data on the transverse noise temperature and the steady drift velocity $\overline{\mathbf{v}}_d$ (48). Values exceeding 20 ps are obtained at low electric fields. As is often the case, the energy relaxation time constant decreases upon carrier heating.

Tensor of Diffusion Coefficients. The first experimental results on diffusion coefficient tensor components for hot majority carriers were obtained using the noise technique (20). The longitudinal and transverse hot-electron noise temperatures were measured at 9.6 GHz for n-type Ge, and the Price relation [Eq. (21)] was used to obtain the electric field dependence of the diffusion coefficient tensor components (see Fig. 4). The transverse component at nonequilibrium was found to exceed its value at equilibrium. The longitudinal component decreases as the electric field increases. As mentioned earlier (see subsection on Convective Noise), the energy fluctuations contribute to the longitudinal rather than the transverse fluctuations [see Eq. (25)]. Consequently, Fig. 4 gives experimental evidence of the negative contribution of the convective noise to the spectral density of longitudinal current fluctuations (11,12).

Comparison to Time-of-Flight Experiment. It would be interesting to compare the results on hot carrier diffusion obtained by the noise technique with those available from other experiments. Time-of-flight technique (see Ref. 33) provides direct observation of longitudinal diffusion. In this technique, a sheet of electrons (or holes) drifts in an electric field in a semi-insulating plate placed into a charged condenser. The shape of the pulse of the condenser discharge current contains information on the average time of flight and its dispersion, the latter being dependent on the sheet spreading, hot-electron diffusion being among other possible causes. Noise and time-of-flight experiments are difficult to perform on exactly the same material, because of almost incompatible requirements inherent in these techniques. Insulating or semi-insulating samples with rectifying contacts are preferable in the time-of-flight experiment, while the noise experiment must be performed on doped (better on lightly doped) samples with ohmic electrodes. As already mentioned, the latter requirements are important for matching the sample to the input circuit of the microwave radiometer, and in order to avoid contribution from shot noise. In spite of these difficulties, a few successful experiments have provided some valuable comparisons. Figure 5 compares the longitudinal tensor components of hot-hole diffusion coefficient available from noise (closed circles) and spreading (open circles) experiments, performed on silicon at 300 K (25). The agreement is good throughout the range of electric fields, where the results are available from both experiments.

Excess Noise Spectra

As a rule, several kinetic processes contribute to longitudinal fluctuations. This leads to rich noise spectra, Lorentz-type contributions appearing as steps at $\omega \ll 1/\tau_m$. So, spectral investigation of excess noise in the current direction deserves

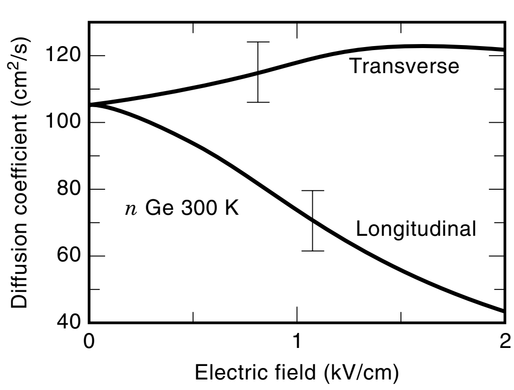

Figure 4. Hot-electron diffusion coefficients differ in the longitudinal and transverse directions to the steady current. Experimental data for n-type germanium (21) ($n = 2 \cdot 10^{14}$ cm^{-3}, $T_0 = 300$ K).

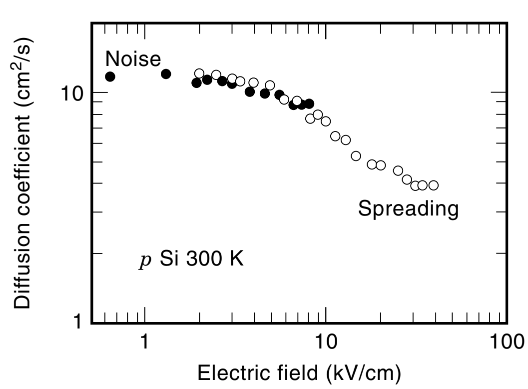

Figure 5. Longitudinal diffusion coefficient of hot holes in silicon at $T_0 = 300$ K: the results obtained from noise experiments (closed circles) match those available from spreading experiments (open circles) (25).

more attention than that in the transverse direction. Hereinafter the focus will be on the longitudinal fluctuations, longitudinal noise, and other longitudinal quantities. For simplicity, the subscript indicating the direction of measurements is omitted.

Generation-Recombination and Intervalley Noise in Silicon. Measurements of noise spectra at low frequencies necessitate application of long pulses of voltage, and the Joule effect limits the range of electric fields where hot electron effects can be investigated experimentally. Figure 6 shows the spectral density of longitudinal current fluctuations measured in ⟨100⟩ direction for *n*-type silicon at 200 V/cm at 78 K temperature (Fig. 6, symbols, see Ref. 24). In addition to $1/f$ noise at low frequencies, two plateaus of the excess noise are resolved in the frequency range below 10 GHz. The fluctuations of electron number in the conduction band dominate at frequencies below 50 MHz, while the hot-electron fluctuations prevail at microwave frequencies. The solid curve is the fitted approximation, assuming 20 ns and 50 ps time constants for two Lorentz-type contributions [see Eq. (15)]. The hot-electron contribution (dashed curve) dominates in the frequency range $\omega\tau_R \gg 1$, where $\tau_R = 20$ ns is the time constant of the generation-recombination process.

Intervalley Noise, Comparison to Monte Carlo Data. Important information on the origin of hot-electron fluctuations in *n*-type Si at $\omega\tau_R \gg 1$ (Fig. 6) follows from comparison (44) of the longitudinal fluctuations measured in two directions of applied electric fields, $\mathbf{E} \parallel \langle 100\rangle$ and $\mathbf{E} \parallel \langle 111\rangle$ (see the open and closed circles in Fig. 7). Due to the conduction band structure of silicon, all valleys are oriented at the same angle to the electric field when the latter is applied along the ⟨111⟩ axis. Consequently, there is no intervalley noise in this configuration, but the intervalley noise is activated when the valleys are made nonequivalent, for example, for $\mathbf{E} \parallel \langle 100\rangle$ [see Eq. (26)].

The results of Monte Carlo simulation of longitudinal velocity fluctuations (49) (Fig. 7, solid lines) give a satisfactory description of the experimental data (Fig. 7, symbols). In the configuration $\mathbf{E} \parallel \langle 111\rangle$ (curve 3 of Fig. 7), corresponding to no intervalley noise, the convective noise leads to a negative contribution due to energy fluctuations at frequencies below $\omega \sim 1/\tau_\epsilon$ (11,12) [see Eq. (25)]. The results of Monte Carlo simulation allow one to estimate the energy relaxation time constant for this configuration: $\tau_\epsilon \approx 15$ ps at $E = 200$ V/cm, $T_0 = 78$ K (curve 3 in Fig. 7).

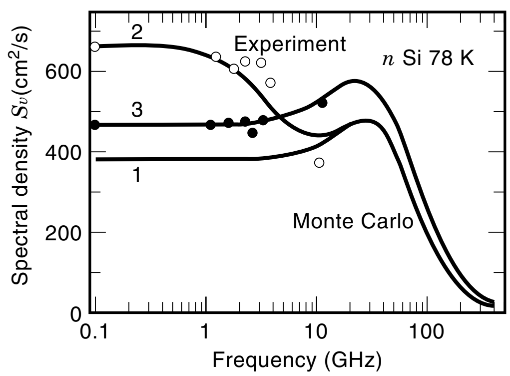

Figure 7. Experimental and simulated spectra of longitudinal velocity fluctuations of hot electrons in *n*-type Si at $T_0 = 78$ K, $E = 200$ V/cm (44) to illustrate the intervalley noise observed at frequencies below 10 GHz for the field **E** applied along ⟨100⟩ axis, and the negative convective-type contribution prevailing at frequencies below 20 GHz for $\mathbf{E} \parallel \langle 111\rangle$. Experimental results: $\mathbf{E} \parallel \langle 100\rangle$ (open circles), $\mathbf{E} \parallel \langle 111\rangle$ (closed circles). Results of Monte Carlo simulation 1—$\mathbf{E} \parallel \langle 100\rangle$, intervalley transitions neglected; 2—$\mathbf{E} \parallel \langle 100\rangle$, intervalley transitions included; 3—$\mathbf{E} \parallel \langle 111\rangle$ the intervalley transitions are included, but they do not contribute because $\bar{v}_1 = \bar{v}_2$; see Eq. (26).

There is a competition of the convective and intervalley noise in the configuration $\mathbf{E} \parallel \langle 100\rangle$. For the energy relaxation time constant in this configuration at $E = 200$ V/cm, $T_0 = 78$ K, one obtains $\tau_\epsilon \approx 5$ ps. The energy relaxation time constant appears to be shorter than the intervalley time constant $\tau_i \approx 50$ ps, and the local minimum is resolved at frequencies $\tau_i^{-1} < \omega = 2\pi f < \tau_\epsilon^{-1}$, as evidenced by the Monte Carlo simulation data (curve 2 in Fig. 7).

As discussed in relation to Fig. 3, the energy relaxation time constant decreases as the electric field increases. The experimental data and the results of Monte Carlo simulation show (18) that the intervalley time constant τ_i in *n*-type Si becomes shorter at a higher electric field as well.

Hot Carrier Effect on Generation-Recombination Noise. The Lorentz-type step at $\omega \sim \tau_R^{-1}$ due to generation-recombination fluctuations shifts toward higher frequencies at higher electric fields, as shown experimentally for *p*-type silicon at 77 K (see Ref. 25). This behavior is caused by the hot-hole effect on generation-recombination noise. Indeed, hole trapping and release probabilities (entering the time constant of the generation-recombination process) depend on the electric field and the hot-hole energy, in particular. For spectral analysis of the noise in *p*-type silicon, including hot-hole velocity fluctuations and the hot-hole effect on generation-recombination fluctuations, see review papers (25,34).

High Electric Fields. The hot-electron noise spectra at moderate fields in the frequency range down to 50 kHz (see Fig. 6) were obtained using long pulses of voltage. However, at high electric fields, the short-time-domain pulsed technique must be used in order to avoid lattice heating. This technique puts the limit on the frequency range: $f \gg 1/\Delta t$, where Δt is the voltage pulse duration. As a result, the experimental

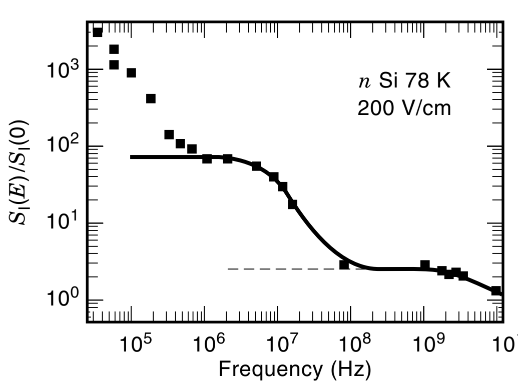

Figure 6. Experimental results on spectral density of longitudinal current fluctuations in *n*-type Si [squares (24)] in the frequency range from 1 MHz to 10 GHz can be described by two Lorentz-type contributions (curves) with the time constants $\tau_R = 20$ ns and $\tau_v = 50$ ps. $S_I \parallel \mathbf{E} \parallel \langle 100\rangle$, $T_0 = 78$ K, $n = 3 \cdot 10^{13}$ cm^{-3}, $E = 200$ V/cm.

noise spectra over the wide range of electric fields are available at high frequencies, usually exceeding 100 MHz (see Refs. 25,29,50).

The experimental results on frequency-dependent longitudinal noise temperature in n-type InP (29) (Fig. 8, symbols) can be interpreted in terms of sources of noise caused by generation-recombination and velocity fluctuations (Fig. 8, solid lines). At X-band microwave frequencies, where the contribution of generation-recombination noise is negligible, the kinetic processes inside the conduction band of InP contribute to the longitudinal noise. Again, 10 GHz frequency proves to be convenient to investigate details of hot-electron noise, its dependence on electric field, sample length, lattice temperature, and semiconductor parameters.

Intervalley Noise in *n*-Type GaAs and InP

Dependence on Intervalley Separation Energy. As is well known, the intervalley separation energy in InP is wider as compared with that of GaAs. Therefore, higher electric fields are required for hot-electron intervalley transfer, and the resultant noise to appear in InP (24,25). The intervalley noise dominates at electric fields over 2 kV/cm in GaAs and over 6 kV/cm in InP (Fig. 9), which are below the threshold field for negative differential mobility due to the intervalley transfer, respectively, around 3.5 kV/cm and 12 kV/cm at 300 K. This is a good illustration that even a small number of high-energy electrons (available, e.g., at $E \sim 6$ kV/cm in InP) is essential for hot-electron noise.

Intervalley Coupling Constants. The intervalley contribution to the spectral density of velocity fluctuations is inversely proportional to the squared intervalley coupling constant [see Eq. (26) and the text following it]. This important parameter of hot-electron intervalley transfer can be estimated by comparing the experimental results with those obtained by model calculations. Monte Carlo simulation (31,51) predicted the intervalley-related maximum of the spectral density of longitudinal velocity fluctuations in n-type InP, to appear at around 8 kV/cm fields. Figure 10 compares the results of simulation with the experimental ones. The experimental results obtained on long samples (crosses 1 in Fig. 10, see Ref. 24) are in a reasonable agreement with those of simulation when the coupling constant $1 \cdot 10^9$ eV/cm is assumed [Fig. 10, solid line, (51)]. A lower value of the coupling constant would be responsible for a longer intervalley time constant and the higher values of the intervalley contribution to $S_v(E)$ [see Eq. (26)], as illustrated by dashed curve 6 in Fig. 10.

The spectral density of intervalley fluctuations in lightly doped n-type GaAs (28) is essentially higher as compared with InP. This comparison suggests a low value of the intervalley coupling constant. The problem was considered in the framework of a three-valley (Γ–L–X) model, and a rather low Γ–L coupling constant, $1.8 \cdot 10^8$ eV/cm, (52) was proposed. The model predicted a strong frequency dependence of S_v at around 10 GHz, which was not confirmed by the experimental

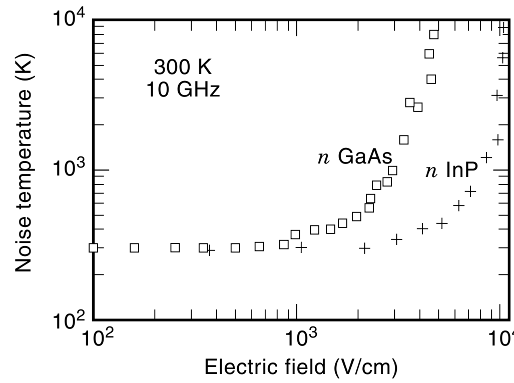

Figure 9. A higher intervalley separation energy causes the intervalley noise to appear at higher fields (24), as illustrated by experimental results on longitudinal noise temperature for n-type GaAs [squares, $\mu_0 = 7500$ cm^2/(V s), $n = 0.9 \cdot 10^{15}$ cm^{-3}] and n-type InP [crosses, $\mu_0 = 4600$ cm^2/(V s), $n = 3.2 \cdot 10^{15}$ cm^{-3}].

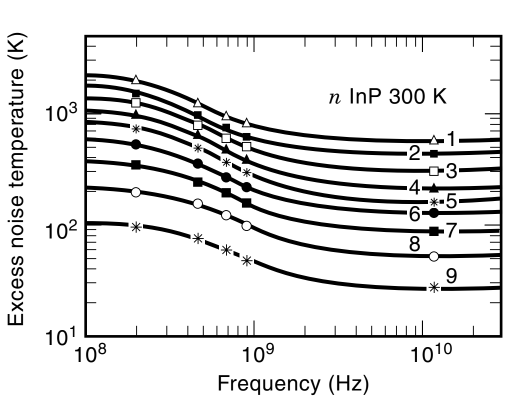

Figure 8. Lorentz-type contributions due to generation-recombination noise (curves) are important at $f < 1$ GHz and are not important at 10 GHz frequency, where the longitudinal excess noise temperature $(T_n)_\parallel - T_0$ results from hot electrons noise. Experimental data on lightly doped n-type InP ($n = 2.7 \cdot 10^{15}$ cm^{-3}) at $T_0 = 300$ K (29) (symbols): 1—10 kV/cm, 2–9 kV/cm, 3—8 kV/cm, 4—7 kV/cm, 5—6 kV/cm, 6—5 kV/cm, 7—4 kV/cm, 8—3 kV/cm, 9—2 kV/cm.

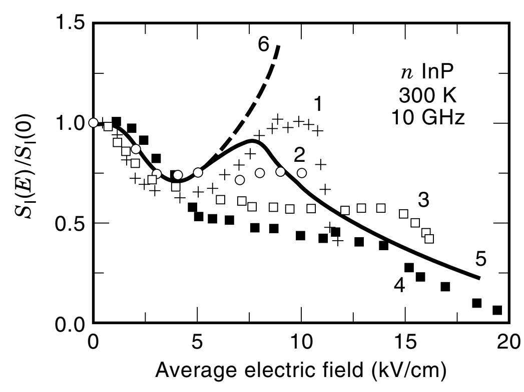

Figure 10. Normalized longitudinal spectral density of current fluctuations depends on sample length in the field range where the intervalley noise dominates in n-type InP. The experimental data on long samples (symbols 1) compared with the results of Monte Carlo simulation (curves 5 and 6) provide an estimate of the intervalley coupling constant. Experimental results for samples of different length L (symbols): 1—L = 10 μm, $n = 3.2 \cdot 10^{15}$ cm^{-3}, $\mu_0 = 4600$ cm^2/(V s) (24), 2—L = 5 μm, $n = 2.7 \cdot 10^{15}$ cm^{-3}, $\mu_0 = 4500$ cm^2/(V s) (28), 3—L = 5 μm, $n = 2.3 \cdot 10^{15}$ cm^{-3}, $\mu_0 = 4600$ cm^2/(V s) (24), 4—L = 1.7 μm, $n = 5.4 \cdot 10^{15}$ cm^{-3}, $\mu_0 = 4600$ cm^2/(V s) (23). Results of Monte Carlo simulation for long samples (46) assuming different intervalley coupling constant (curves): 5—$1 \cdot 10^9$ eV/cm; 6—$3 \cdot 10^8$ eV/cm.

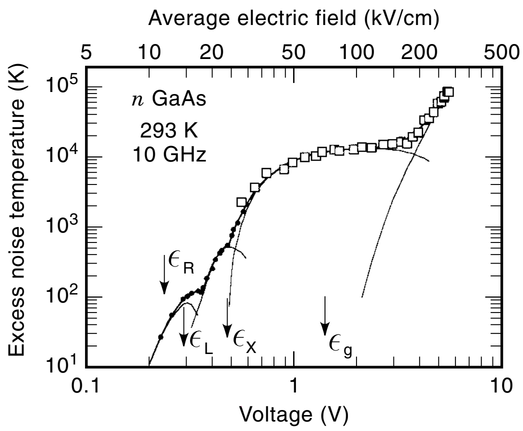

Figure 11. Four sources of hot-electron noise (activated at different threshold energies) are resolved in n-type GaAs channel of submicrometer length ($n = 3 \cdot 10^{17}$ cm^{-3}, $L = 0.2$ μm) at $T_0 = 293$ K (30). Voltage pulse duration: 2 μs (dots), 100 ns (squares). Solid curve stands for the sum of the contributions given by the thin curves.

data (50), and an intermediate value of the Γ–L coupling constant, $3 \cdot 10^8$ eV/cm, was assumed to avoid contradictions of the three-valley model with the experimental data (see Ref. 24) and references therein].

Intervalley Noise Due to L- and X-Valleys in GaAs. Sources of hot-electron noise with threshold energies corresponding to the L- and X-valleys in n-type GaAs are resolved using nanosecond pulses of voltage applied to short channels. Figure 11 shows the excess noise temperature $\Delta T_n = T_n - T_0$, plotted as a function of voltage V at $T_0 = 293$ K ambient temperature (30). The channel length being 0.2 μm, the average fields up to 300 kV/cm are reached in standard-doped GaAs channels ($3 \cdot 10^{17}$ cm^{-3}). The steep increase in current accompanies the increase in noise temperature at the highest fields—an experimental evidence for the impact ionization noise of hot electrons resolved in a conduction channel.

The $\Delta T_n(V)$ dependence can be decomposed into four sources of hot-electron noise: thin lines in Fig. 11 indicate possible contributions of each source. The lowest threshold appears at around 0.2 V; it results from the resonant scattering of hot-electrons by the impurity levels located inside the conduction band (53) (see also Ref. 54). The thresholds at 0.3 V and 0.5 V result from scattering of almost ballistically accelerated electrons into the L- and X-valleys of the conduction band (the L- and X-valley energies are close to 0.3 eV and 0.5 eV, respectively). The extrapolation of the experimental data on $\Delta T_n(V)$ obtained at the highest average fields yields the threshold energy for the impact ionization noise; the threshold energy, as expected, exceeds the forbidden gap.

The quasi-saturation of hot-electron noise temperature takes place at the average electric fields, ranging from 50 kV/cm to 200 kV/cm. This very specific noise behavior has been used to estimate the time constant for the Γ–X transfer experienced by the high-energy electrons present in the Γ-valley at the energy $\epsilon > \epsilon_X \approx 0.5$ eV: 30 fs $< \tau_{\Gamma X} <$ 60 fs (30). This estimate, based on the hot-electron noise data, provides an independent confirmation of the results available from femtosecond and cw luminescence data.

Suppression of Hot-Electron Noise in Short Samples

Time and space are needed for the complete development of fluctuations, and hot-electron noise depends on sample dimensions. Indeed, a hot electron spends limited time in a short sample and cannot acquire the energy accessible in a longer sample. Since the tail of the autocorrelation function [see Eq. (3)] is cut off, Eq. (4) leads to lower values of the spectral density. Hence, sources of noise caused by relatively slow kinetic processes and/or appearing at high threshold energies are suppressed in short samples. In other words, threshold-type sources of noise appear at higher electric fields in short samples.

Suppression of Intervalley Noise. Figure 12 illustrates the length-dependent behavior of hot-electron noise in lightly doped n-type GaAs (40). There is no dependence of the noise temperature T_n on sample length L in long samples (symbols 1 and 2 of Fig. 12). However, the same noise temperature requires essentially higher electric fields in short samples (see symbols 2 and 3, 4 in Fig. 12). For a fixed average electric field, say $V/L = 3$ kV/cm, the noise suppression exceeds 10 dB as the sample length L is reduced from 7.5 μm (symbols 2) to 1.5 μm (symbols 3).

A detailed interpretation of suppression is reached by comparing the experimental results with those obtained by Monte Carlo simulation. Figure 13 presents the spectral density of current fluctuations $S_I(E)$ normalized to its value at zero bias $S_I(0)$. The experimental data for n-type GaAs are presented by open symbols from 1 to 4. As noted earlier, the main source of current fluctuations in long samples at fields over 2 kV/cm results from hot-electron intervalley transfer. This source of fluctuations is heavily suppressed in a 1 μm sample (Fig. 13, points 4): the monotonously increasing dependence on electric field changes into a monotonously decreasing one, typical for one-valley semiconductors. Closed symbols in Fig. 13 correspond to Monte Carlo simulation of hot-electron fluctua-

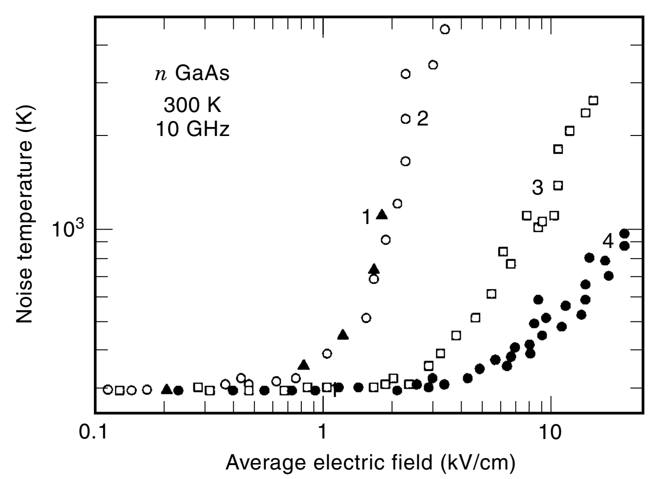

Figure 12. Suppression of the intervalley noise in short samples as illustrated by experimental results on longitudinal noise temperature of hot electrons in n-type GaAs at room temperature (28,40). Samples length and other data: 1—$L = 1000$ μm, $\mu_0 = 6000$ cm^2/(V s), 2—$L = 7.5$ μm, $n = 10^{15}$ cm^{-3}, $\mu_0 = 7500$ cm^2/(V s). 3—$L = 1.5$ μm, $n = 10^{15}$ cm^{-3}, $\mu_0 = 7500$ cm^2/(V s). 4—$L = 1$ μm, $n = 10^{15}$ cm^{-3}, $\mu_0 = 7500$ cm^2/(V s).

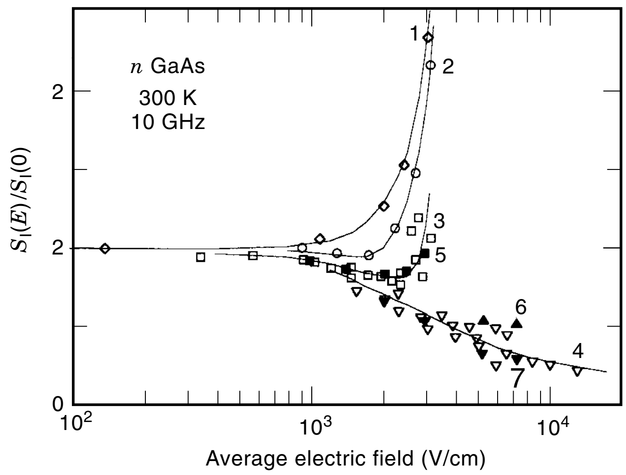

Figure 13. Transition from the monotonously increasing (diamonds 1) to the monotonously decreasing (open triangles 4) dependence on electric field of the normalized longitudinal spectral density of current fluctuations, illustrating suppression of the intervalley fluctuations in short (micrometer) samples. Experimental results correspond to lightly doped n-type GaAs (open symbols, curves are to guide the eye): 1—$L = 1000$ μm, $\mu_0 = 6000$ cm^2/(V s) (28); 2—$L = 11$ μm, $\mu_0 = 5200$ cm^2/(V s) (45); 3—$L = 7.5$ μm, $\mu_0 = 7500$ cm^2/(V s) (37), 4—$L = 1$ μm, $\mu_0 = 7500$ cm^2/(V s) (37). Monte Carlo simulation data (closed symbols) correspond to different values of sample length and Γ-L intervalley coupling constant (50): 5—$L = 7.5$ μm, $1.8 \cdot 10^8$ eV/cm, 6—$L = 1$ μm, $1.8 \cdot 10^8$ eV/cm, 7—$L = 1$ μm, $1 \cdot 10^9$ eV/cm.

tions (55) (nonuniformity of the electric field and space charge fluctuations are taken into account). There is a reasonable agreement between the results of experiment and simulation.

In a similar way, the hot-electron intervalley fluctuations observed in long samples of n-type InP at fields over 6 kV/cm are suppressed in short samples (Fig. 10). Indeed, the maximum of spectral density in 10 μm samples (Fig. 10, crosses 1) diminishes and disappears as the sample length L is reduced down to 1.7 μm (symbols 4).

Critical Length for Noise Suppression. Under steady flow of current, hot electrons are constantly leaving the sample, and equilibrium electrons are entering at the cathode. This "exchange" opens an additional (external) energy loss mechanism by the hot electrons present in the sample. The external loss is negligible, as compared with the internal loss in long samples, but its relative weight increases when the sample length L is reduced. At a certain critical length the external loss assumes primary importance. It is evident that the critical length is shorter, provided the internal loss is greater.

Figure 14 compares the hot-electron noise temperature at a fixed average electric field, $V/L = 4$ kV/cm, for GaAs samples of different length and doping (53). The results can be interpreted in terms of the critical lengths required for the electrons to gain the threshold energy of the dominant source of noise. The curves in Fig. 14 assume two critical lengths used as fitting parameters: L_1 stands for the lucky electrons, which do not undergo scattering events before they reach the threshold energy, and L_2 takes into account energy loss during electron acceleration to the same threshold energy. The curves correspond to $L_1 = 1.3$ μm, $L_2 = 3$ μm for lightly doped (curve 1, Fig. 14) and to $L_1 = 0.3$ μm, $L_2 = 0.2$ μm for standard-doped GaAs (curve 2). The critical lengths are shorter and the threshold energies are lower in the standard-doped GaAs channels.

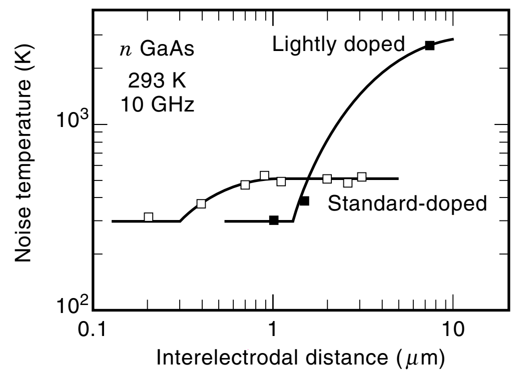

Figure 14. Suppression of hot-electron noise in short channels: essentially shorter lengths are needed for the suppression in the standard-doped n-type GaAs, as compared with the lightly doped samples, provided the same average electric field $V/L = 4$ kV/cm is applied (53). Open squares—$n = 3 \cdot 10^{17}$ cm^{-3}, $\mu_0 = 4000$ cm^2/(V s), closed squares—$n = 3 \cdot 10^{15}$ cm^{-3}, $\mu_0 = 7500$ cm^2/(V s); solid curves are fitted approximations based on concepts of ballistic and dissipative critical lengths.

Transition from Shot Noise to Hot-Electron Noise

So far uniformly doped samples with ohmic electrodes have been considered. These conditions favoring hot-electron noise rather than shot noise. However, most electronic devices contain barriers formed by nonuniform doping, surface charges, and heterojunctions. According to the Schottky formula (5) the spectral density of longitudinal current fluctuations due to shot noise increases proportionally to the constant current, while the corresponding dependence is steeper for hot electrons. In a diode, the shot noise prevails at low currents, but a transition to hot-electron noise can occur at high currents, unless the thermal breakdown takes place before the critical current is reached. The thermal breakdown has been avoided and the transition in question is observed in GaAs Schottky and planar-doped barrier diodes at high forward currents, by using short-time-domain radiometry of the noise power (56).

Figure 15 presents the spectral density of current fluctuations, S_I, measured (56) at 10 GHz frequency for the forward-

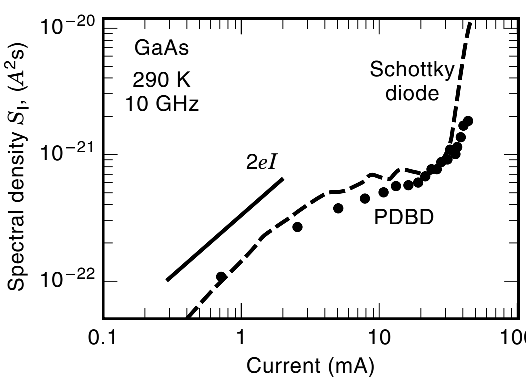

Figure 15. Spectral density of longitudinal current fluctuations of GaAs diodes demonstrates transition from shot noise to hot-electron noise at high forward currents (56). Schottky diode (dashed line) and planar-doped barrier diode (PDBD, closed circles). Solid line is the Schottky formula for shot noise $S_I = 2eI$.

biased GaAs Schottky diode and planar-doped barrier diode (PDBD). The measured spectral density is almost proportional to the current at very low current levels (Fig. 15), when the barrier controls the current and the shot noise dominates. The experimental points are close to the solid line (Fig. 15) standing for the Schottky formula $S_I = 2eI$. The sublinear dependence of $S_I(I)$ indicates onset of the screening effect of space charge of drifting electrons. Eventually, at high currents, the sublinear dependence becomes superlinear. This change of the dominant source of fluctuations is accompanied by an onset of a different electron transport mechanism: the barrier diminishes and fails to control the current flow. These results give experimental evidence for transition to hot-electron dominated noise in GaAs Schottky and planar-doped barrier diodes.

Noise in 2-DEG Channels

Modern heterostructure growth technology provides a great variety of AlGaAs/GaAs, InAlAs/InGaAs, InP/InGaAs channels for lattice-matched and pseudomorphic high electron mobility transistors (HEMT and PHEMT), containing two-dimensional electron gas (2-DEG) confined in the quantum well (QW). High mobility of confined electrons is advantageous for fast operation of 2-DEG channels. However, electron heating by an electric field applied along the channel is accompanied by enhanced chaotic motion of hot electrons in the plane of electron confinement, occupation of upper subbands, hot-electron deconfinement (real-space transfer) and other kinetic processes specific to a hot two-dimensional electron gas. The associated longitudinal fluctuations appear in QW channels [see Ref. (44)]. Hot-electron velocity fluctuations due to real space transfer have been resolved first in selectively doped AlGaAs/GaAs channels (40). The experimental results are in reasonable agreement with the results of Monte Carlo simulation (57). Moreover, the threshold field for this noise source increases as the heterobarrier height increases (58,59). This supports the idea of transverse real-space transfer being responsible, among other factors, for the longitudinal fluctuations of current. A special case of real-space transfer is transverse tunneling of hot electrons across a thin barrier of AlAs, separating the 2-DEG channel and the ionized donors in AlGaAs/GaAs/AlAs/GaAs structure. The associated longitudinal fluctuations are heavily suppressed in short channels (60). The intersubband noise appears in δ-doped GaAs channels, where the upper subbands support higher electron mobilities as compared with more confined electronic states of the lower subbands. Dependence of hot-electron noise on the quantum well shape (61) is important in quasi-triangular and quasi-rectangular quantum wells in InAlAs/InGaAs/InAlAs channels. These heterostructures can be heavily doped, in order to obtain high-density 2-DEG useful for high-power applications. Heavy doping of the structures is accompanied by the excess fluctuations (62) absent in the low-density 2-DEG.

Real-Space Transfer Noise. Figure 16 compares (59) the spectral density of longitudinal current fluctuations in GaAs samples and AlGaAs/GaAs single-heterojunction 2-DEG channels. The local maximum of the spectral density appears (Fig. 16, squares and circles) at the intermediate fields 100 V/cm $< E <$ 2 kV/cm, which are low, as compared with the intervalley transfer field in GaAs. The height and position

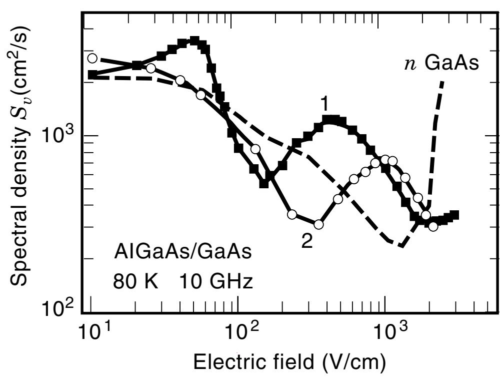

Figure 16. Spectral density of longitudinal velocity fluctuations in AlGaAs/GaAs quantum well channels gives an experimental evidence for sources of fluctuations specific to two-dimensional electron gas (symbols) absent in GaAs samples (dashed curve) (58). Al mole ratio in the spacer: 1—25% Al, $n = 6 \cdot 10^{11}$ cm^{-2}, $\mu_0 = 75000$ cm^2/(V s), 2—33% Al, $n = 2 \cdot 10^{11}$ cm^{-2}, $\mu_0 = 103000$ cm^2/(V s). Dashed line is for n-type GaAs [$n = 9 \cdot 10^{14}$ cm^{-3}, $\mu_0 = 77000$ cm^2/(V s)]. Solid curves are guides to the eye.

of the maximum depend on the Al mole ratio in the selectively doped AlGaAs layer: the source of fluctuations in question appears at a higher field (circles 2 in Fig. 16), when the heterobarrier is higher. This is strong experimental evidence for hot-electron jumps from the QW into the AlGaAs layer and backwards. The experimental data also show that this real-space transfer suppresses the intervalley fluctuations of hot electrons dominating in GaAs at fields over 2 kV/cm (see symbols and solid line in Fig. 16). The shape of the maximum is similar to that obtained by Monte Carlo simulation of the real-space transfer fluctuations (57), as illustrated by Fig. 17.

Interpret the maximum observed at 1 kV/cm field (Fig. 17, circles) in terms of Eq. (26). Since electron mobility is high in the quantum well channel and low in the adjacent doped layer of AlGaAs, the electron drift velocities $\bar{v}_1$ and $\bar{v}_2$ differ. The increase in electric field causes the monotonous decrease of electron density in the QW (the ratio $\bar{n}_1/\bar{n}_2$ decreases), and

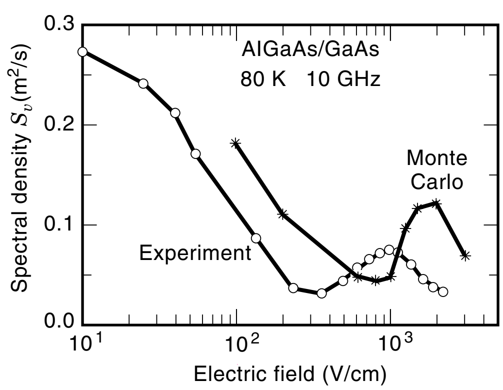

Figure 17. Real-space transfer in AlGaAs/GaAs channel causes the maximum of spectral density of longitudinal velocity fluctuations appearing at electric fields well below those for the intervalley transfer. Open circles stand for the experimental results (59): AlGaAs/GaAs, 33% Al, $n = 2 \cdot 10^{11}$ cm^{-2}, $\mu_0 = 103000$ cm^2/(V s), $T_0 = 80$ K. Stars stand for the results of Monte Carlo simulation for a simplified model of a quantum well channel (52). Solid lines are guides to the eye.

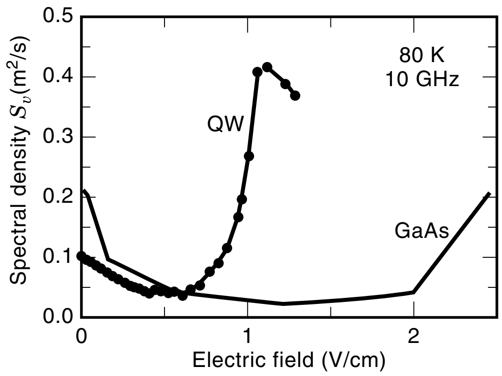

Figure 18. Contribution of transverse tunneling through a thin barrier of AlAs to the spectral density of hot-electron longitudinal velocity fluctuations, appearing in AlGaAs/δ-GaAs/AlAs/GaAs quantum well (QW) channel at electric fields well below those for the intervalley transfer (60). Experimental data for the QW channel [closed circles, $n = 1.3 \cdot 10^{12}$ cm^{-2}, $\mu_0 = 35000$ cm^2/(V s), $T_0 = 80$K] are compared with those for bulk n-type GaAs (see Fig. 16).

the maximum of spectral density forms at around $\overline{n}_1 \approx \overline{n}_2$ [see Eq. (26)]. Under assumption that $\overline{v}_1 - \overline{v}_2 \sim 10^7$ cm/s and $\overline{n}_1 \approx \overline{n}_2$, the real-space transfer time constant is estimated from the maximum value of the spectral density: $\tau \sim 5$ ps (59). The obtained time constant is short; this enables observation of the real-space transfer at 10 GHz frequency and supports the idea of reversible real-space transfer.

Longitudinal Fluctuations Due to Transverse Tunneling. A triple-heterojunction AlGaAs/δ-GaAs/AlAs/GaAs structure has been designed (60) to separate the 2-DEG channel from the doped layer by the thin layer of AlAs. Strong excess noise appears (60) at electric fields well below those for the intervalley transfer (Fig. 18, symbols). The barrier of AlAs is high and thin; therefore, electron jumps over the barrier are excluded, but the high-energy electrons can penetrate it by tunneling. It has been concluded (60) that transverse tunneling is responsible for the steep increase in the longitudinal hot-electron noise temperature (Fig 19, open circles) and the

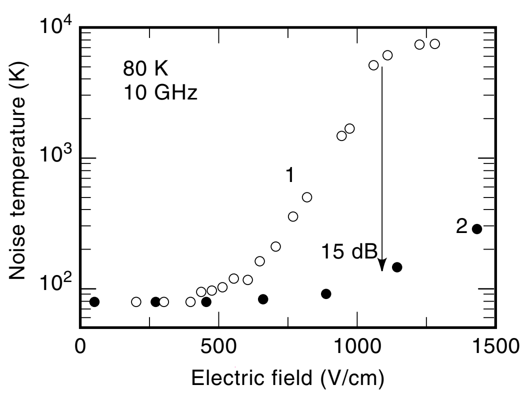

Figure 19. Experimental evidence for suppression (up to 15 dB at 1.1 kV/cm) of the longitudinal noise due to transverse tunneling of hot electrons in short AlGaAs/δ-GaAs/AlAs/GaAs QW channels at 80 K (60). Channel length: 1 to 18 μm, 2 to 3 μm. For the Hall effect data, see Fig. 18.

maximum of spectral density of longitudinal velocity fluctuations (Fig. 18, closed circles) resolved at a field around 1 kV/cm at 80 K lattice temperature. In the framework of Eq. (26) under assumption $\overline{v}_1 - \overline{v}_2 \sim 2 \cdot 10^7$ cm/s, the time constant for the transverse tunneling is estimated to be $\tau \sim 10$ ps (60).

The transverse-tunneling-related noise source observed in a 18 μm channel at a 1 kV/cm field (open circles 1 in Fig. 19) is very weak in the 3 μm channel (closed circles 2). This strong dependence on channel length, being an illustration of suppression of hot-electron noise in short channels, suggests a way for an independent estimate of the transverse tunneling time constant using the electron transit time. The values for tunneling time constant estimated from these two independent experiments are in reasonably good agreement (60). Similar results on the tunneling time constant are available from luminescence data for resonant tunneling, while the nonresonant tunneling time constants are essentially longer.

SUMMARY

Hot carrier noise in semiconductors, being a special case of nonequilibrium noise, does not obey the fluctuation–dissipation theorem and other relations valid for electron gas at thermal equilibrium. Characteristics of hot-electron noise cannot be predicted from data on electron density and mobility measured at low electric fields: the noise spectra at high electric fields display features resulting from subtle details of semiconductor band structure and scattering mechanisms. Experimental investigation of these features at microwave frequencies, together with Monte Carlo simulation, provide the possibility to determine parameters (time constants, coupling constants, etc.) of fast kinetic processes in the conduction (or valence) band of a semiconductor subjected to a high electric field. Suppression of hot-electron noise, favoring low-noise operation of short channels at microwave frequencies, is shown experimentally and through Monte Carlo simulation. A great variety of diverse sources of noise being resolved in low-dimensional channels demonstrates diagnostic possibilities of short-time-domain radiometry of hot-electron noise and high potentials of nanometric technology for development of high-speed, low-noise devices for electronics.

BIBLIOGRAPHY

1. H. Nyquist, Thermal agitation of electric charge in conductors, *Phys. Rev.,* **32** (1): 110–113, 1928.
2. H. B. Callen and T. A. Welton, Irreversibility and generalized noise, *Phys. Rev.,* **83** (1): 34–40, 1951.
3. A. van der Ziel, *Noise in Solid State Devices and Circuits,* New York: Wiley, 1986.
4. Sh. Kogan, *Electronic Noise and Fluctuations in Solids,* Cambridge, U.K.: Cambridge University Press, 1996.
5. N. B. Lukyanchikova, *Noise Research in Semiconductor Physics,* in B. K. Jones (ed.), Amsterdam: Gordon and Breach Science Publs, 1997.
6. W. Schottky, Über spontane Stromschwankungen in verschiedenen Elektrizitätleitern, *Ann. Phys.,* **57**: 541, 1918.
7. E. M. Lifshitz and L. P. Pitaevski, *Physical Kinetics,* Oxford, UK: Pergamon, 1981.
8. M. Lax, Fluctuations from the nonequilibrium steady state, *Revs. Mod. Phys.,* **32** (1): 25–64, 1960.

9. P. J. Price, Intervalley noise, *J. Appl. Phys.,* **31** (6): 949–953, 1960.
10. V. L. Gurevich, On current fluctuations in semiconductors near nonequilibrium steady state, *Zh. Eksp. Teor. Fiz.,* **43** (5): 1771–1781, 1962 (*Sov. Phys.—JETP,* **16** (5): 1252, 1963).
11. P. J. Price, Fluctuations of hot electrons, *Fluctuation Phenomena in Solids,* R. E. Burgess (ed.), New York: Academic Press, 1965, pp. 355–379.
12. V. L. Gurevich and R. Katilius, Theory of hot electrons in an anisotropic semiconductor, *Zh. Eksp. Teor. Fiz.,* **49** (4): 1145–1156, 1965 (*Sov. Phys.—JETP,* **22** (4): 796, 1965).
13. Sh. M. Kogan and A. Ya. Shul'man, Electric fluctuations in solid-state plasma at high electric fields, *Fiz. Tverd. Tela.,* **9** (8): 2259–2264, 1967 (*Sov. Phys.—Solid State,* **9** 1771, 1968).
14. S. V. Gantsevich, V. L. Gurevich, and R. Katilius, Current fluctuations in a semiconductor in high electric field, *Fiz. Tverd. Tela.,* **11** (2): 308–315, 1969 (*Sov. Phys.—Solid State,* **11** (2): 247, 1969).
15. S. V. Gantsevich, V. L. Gurevich, and R. Katilius, Fluctuations in semiconductor in strong electric field and light scattering from hot electrons, *Zh. Eksp. Teor. Fiz.,* **57** (2): 503–519, 1969 (*Sov. Phys.—JETP,* **30** (2): 276, 1970).
16. Sh. M. Kogan and A. Ya. Shul'man, Theory of fluctuations in nonequilibrium electron gas, *Zh. Eksp. Teor. Fiz.,* **56** (3): 862–876, 1969 (*Sov. Phys.—JETP,* **29** (3): 467, 1969).
17. S. V. Gantsevich, V. L. Gurevich, and R. Katilius, Theory of fluctuations in nonequilibrium electron gas, *Rivista del Nuovo Cimento,* **2** (5): 1–87, 1979.
18. V. Bareikis et al., Fluctuation spectroscopy of hot electrons in semiconductors. In *Spectroscopy of Nonequilibrium Electrons and Phonons,* C. V. Shank and B. P. Zakharchenya (eds.), Amsterdam: Elsevier, 1992, pp. 327–396.
19. E. Erlbach and J. B. Gunn, Noise temperature of hot electrons in germanium, *Phys. Rev. Lett.,* **8** (7): 280–282, 1962.
20. C. A. Bryant, Noise temperature of hot electrons in gallium-arsenide, *Bull. Am. Phys. Soc.,* **9** (1): 62, 1964.
21. V. Bareikis, I. Vaitkevičiūtė, and J. Požela, Fluctuations of hot current carriers in germanium, *Liet. Fiz. Rink.,* **6** (3): 437–440, 1966.
22. V. Bareikis, J. Pozhela, and I. Matulionienė, Noise and diffusion of hot carriers in p-Ge, in *Proc. 9th Int. Conf. Physics Semicond.,* S. M. Ryvkin (ed.), Leningrad: Nauka, 1968, pp. 760–765.
23. L. Huxley and R. Crompton, *The Diffusion and Drift of Electrons in Gases,* New York: Wiley, 1974.
24. V. Bareikis et al., Experiments on hot electron noise in semiconductor materials for high-speed devices. *IEEE Trans. Electron Devices,* **41**: 2050–2060, 1994.
25. J. P. Nougier, Fluctuations and noise of hot carriers in semiconductor materials and devices, *IEEE Trans. Electron Devices,* **41**: 2034–2049, 1994.
26. V. Bareikis et al., Noise and diffusivity of hot electrons in n-type InSb, *J. de Physique,* **4** (10): Col. C7, Suppl., C7-215-220, 1981.
27. L. G. Hart, High field current fluctuations in n-type germanium, *Can. J. Phys.* **48** (5): 531–542, 1970.
28. V. Bareikis et al., Microwave noise and the coupling constant for Γ and L valleys in the three-valley model of GaAs, *Fiz. Techn. Polupr.,* **14** (7): 1427–1429, 1980 (*Sov. Phys. Semicond.,* **14** 847, 1980).
29. D. Gasquet, M. Fadel, and J. P. Nougier, Noise of hot electrons in indium phosphide, in *Proc. 7th Inf. Conf. Noise Physical Syst. 1/f Fluctuations,* M. Savelli, G. Lecoy, and J. P. Nougier (eds.), Amsterdam: North Holland, 1983, pp. 169–171.
30. V. Aninkevičius et al., Γ-X intervalley-scattering time constant for GaAs estimated from hot-electron noise spectroscopy data, *Phys. Rev. B.,* **53** (11): 6893–6895, 1996.
31. G. Hill, P. N. Robson, and W. Fawcett, Diffusion and the power density fluctuations for electrons in InP by Monte-Carlo methods, *J. Appl. Phys.,* **50** (1): 356–360, 1979.
32. V. Bareikis et al., Calculation of noise in p-type Ge in a high electric field by the Monte-Carlo method, *Fiz. Techn. Polupr.,* **13** (6): 1123–1126, 1979 (*Sov. Phys.-Semicond.,* **13**: 658, 1979).
33. C. Jacoboni and P. Lugli, *The Monte Carlo Method for Semiconductor Device Simulation,* Vienna: Springer-Verlag, 1989.
34. L. Varani and L. Reggiani, Microscopic theory of electronic noise in semiconductor unipolar structures, *Rivista del Nuovo Cimento,* **17**, ser. 3 (7): 1–110, 1994.
35. T. Kuhn et al., Monte Carlo method for the simulation of electronic noise in semiconductors, *Phys. Rev. B,* **42**: 5702–5713, 1990.
36. L. Reggiani et al., Modelling of small-signal response and electronic noise in semiconductor high-field transport, *Semicond. Science Technol.,* **12**: 141–156, 1997.
37. S. Dedulevich, Zh. Kancleris, and A. Matulis, Fluctuations and diffusion in a weakly heated electron gas, *Zh. Eksp. Teor. Fiz.,* **95** (5): 1701–1710, 1989 (*Sov. Phys.*—JETP, **68** (5): 982–987, 1989).
38. L. Varani, Contribution of interparticles correlations to electronic noise in semiconductors, in *Proc. 13th Int. Conf. Noise in Physical Systems and 1/f Fluctuations,* V. Bareikis and R. Katilius (eds.), Singapore: World Scientific, 1995, pp. 203–208.
39. A. Matulionis, R. Raguotis, and R. Katilius, Interparticle collisions and hot-electron velocity fluctuations in GaAs at 80 K, *Phys. Rev. B,* **56** (4): 2052–2057, 1997.
40. V. Bareikis et al., Velocity overshoot and suppression of diffusivity and microwave noise in short $n^+ - n - n^+$ structures of GaAs, in: *High-Speed Electronics,* B. Källbäck and H. Beneking (eds.), Berlin: Springer, 1986, pp. 28–31.
41. V. Bareikis et al., Long-range fluctuations of hot electrons in GaAs and InP at 80 K, in *Proc. 10th Int. Conf. Noise Physical Syst. 1/f Fluctuations,* A. Ambrozy (ed.), Budapest: Akademiai Kiado, 1990, pp. 53–56.
42. V. Bareikis et al., Length dependent hot electron noise in doped GaAs, *Solid-State Electronics,* **32** (12): 1647–1650, 1989.
43. V. Aninkevičius et al., Real-space-transfer noise and diffusion in GaAs/AlGaAs heterostructure, in *Proc. 11th Int. Conf. Noise Physical Syst. 1/f Fluctuations,* T. Musha, S. Sato, and M. Yamamoto (eds.), Tokyo: Ohmsha, 1991, pp. 183–186.
44. V. Bareikis, R. Katilius, and A. Matulionis, High-frequency noise in heterostructures, in *Proc. 13th Int. Conf. Noise Physical Syst. 1/f Fluctuations,* V. Bareikis and R. Katilius (eds.), Singapore: World Scientific, 1995, pp. 14–21.
45. P. Shiktorov et al., Noise temperature of n+nn+ GaAs structures, *Phys. Rev. B,* **54**: 8821–8832, 1996.
46. C. W. Gardiner, *Quantum Noise,* Berlin: Springer-Verlag, 1991.
47. R. Šaltis, Soviet Patent 248063. Gate modulated meter of weak pulse signals with the alternating coefficient of filing (in Russian), *Bulletin Izobretenij,* Nb.23, 1969.
48. V. A. Bareikis, A. P. Galdikas, and J. K. Požela, Noise, time of energy relaxation and diffusion of hot holes in p-germanium in the magnetic field, *Fiz. Techn. Polupr.,* **11** (2): 365–372, 1977 (*Sov. Phys.—Semicond.,* **11**: 210, 1977).
49. V. Bareikis, V. Viktoravičius, and A. Galdikas, Noise dependence upon frequency in n-Si at high electric fields, *Fiz. Techn. Polupr.,* **16** (10): 1868–1870, 1982 (*Sov. Phys.—Semicond.,* **16**: 1202, 1982).

50. D. Gasquet et al., Diffusion noise of hot electrons in GaAs at 300 K, in *Proc. Int. Conf. Noise Physical Syst. 1/f Noise,* A. d'Amico and P. Mazzetti (eds.), Amsterdam: Elsevier, 1985, pp. 227–230.
51. C. Hammar and V. Vinter, Diffusion of hot electrons in indium phosphide, *Electronics Lett.,* **9** (1): 9–10, 1973.
52. J. Požela and A. Reklaitis, Diffusion coefficient of hot electrons in GaAs, *Solid State Communications.,* **27** (11): 1073–1077, 1978.
53. V. Bareikis et al., Impurity resonant scattering of hot electrons in GaAs, in *Proc. 20th Int. Conf. Physics Semiconductors,* E. M. Anastassakis and J. D. Joannopoulos (eds.), Singapore, World Scientific, 1990, p. 2479–2482.
54. A. Matulionis et al., Microwave- and low-frequency fluctuations caused by DX-centres in GaAs and AlGaAs, in *Proc. 14th Int. Conf. Noise Physical Syst. 1/f Fluctuations,* C. Claeys and E. Simoen (eds.), Singapore: World Scientific, 1997, pp. 453–456.
55. D. Junevičius and A. Reklaitis, Monte Carlo particle investigations of noise in short $n^+ - n - n^+$ GaAs diodes, *Electron. Lett.,* **24** (21): 1307–1308, 1988.
56. J. Liberis et al., Microwave noise in unipolar diodes with nanometric barriers, in *Proc. 14th Int. Conf. Noise Physical Syst. 1/f Fluctuations,* C. Claeys and E. Simoen (eds.), Singapore: World Scientific, 1997, pp. 67–70.
57. J. Zimmermann and Y. Wu, Diffusion coefficients of two-dimensional electron gas in heterojunctions, *Solid-State Electronics,* **31** (3/4): 367–370, 1988.
58. V. Aninkevičius et al., Comparative analysis of microwave noise in GaAs and AlGaAs/GaAs channels, *Solid-State Electronics,* **36** (9): 1339–1343, 1993.
59. V. Aninkevičius et al., Hot electron noise and diffusion in AlGaAs/GaAs, *Semicond. Sci. Technol.,* **9** (5S): 576–579, 1994.
60. V. Aninkevičius et al., Transverse tunnelling time constant estimated from hot-electron noise in GaAs-based heterostructure, *Solid State Commun.,* **98** (11): 991–995, 1996.
61. A. Matulionis et al., QW-shape-dependent hot-electron velocity fluctuations in InGaAs-based heterostructures, *Physica Status Solidi (b),* **204** (1): 453–456, 1997.
62. V. Aninkevičius et al., Hot electron noise in InAlAs/InGaAs/InAlAs quantum wells, in *Proc. 14th Int. Conf. Noise Physical Syst. 1/f Fluctuations,* C. Claeys and E. Simoen (eds.), Singapore: World Scientific, 1997, pp. 71–74.

ARVYDAS MATULIONIS
Semiconductor Physics Institute